



HAL
open science

A new ichnofauna from the Permian of the Zat Valley in the Marrakech High Atlas of Morocco

Jean-David Moreau, Naima Benaouiss, Abdelilah Tourani, J.-Sébastien Steyer, Michel Laurin, Karin Peyer, Olivier Bethoux, Ali Aouda, Nour-Eddine Jalil

► **To cite this version:**

Jean-David Moreau, Naima Benaouiss, Abdelilah Tourani, J.-Sébastien Steyer, Michel Laurin, et al.. A new ichnofauna from the Permian of the Zat Valley in the Marrakech High Atlas of Morocco. *Journal of African Earth Sciences*, 2020, pp.103973. 10.1016/j.jafrearsci.2020.103973 . mnhn-02922570

HAL Id: mnhn-02922570

<https://mnhn.hal.science/mnhn-02922570>

Submitted on 5 Sep 2022

HAL is a multi-disciplinary open access archive for the deposit and dissemination of scientific research documents, whether they are published or not. The documents may come from teaching and research institutions in France or abroad, or from public or private research centers.

L'archive ouverte pluridisciplinaire **HAL**, est destinée au dépôt et à la diffusion de documents scientifiques de niveau recherche, publiés ou non, émanant des établissements d'enseignement et de recherche français ou étrangers, des laboratoires publics ou privés.



Distributed under a Creative Commons Attribution - NonCommercial 4.0 International License

1 **A new ichnofauna from the Permian of the Zat Valley in the Marrakech**
2 **High Atlas of Morocco**

3

4 Jean-David Moreau^{a*}, Naima Benaouiss^b, Abdelilah Tourani^b, J.-Sébastien Steyer^c, Michel
5 Laurin^c, Karin Peyer^c, Olivier Béthoux^c, Ali Aouda^d, Nour-Eddine Jalil^{b, c}

6

7 ^aUMR CNRS 6282 Biogéosciences, Université de Bourgogne Franche-Comté, 6 boulevard
8 Gabriel, 21000 Dijon, France.

9 ^bDépartement de géologie, Faculté des Sciences Semlalia, Université Cadi Ayyad, BP 2390,
10 Marrakech 40000, Morocco.

11 ^cCentre de Recherches en Paléontologie – Paris (CR2P), UMR 7207,
12 CNRS/MNHN/SU/EPHE, Muséum national d'Histoire naturelle, Paris, France.

13 ^dLaboratoire des études sur les ressources, la mobilité et l'attractivité, Faculté des lettres et des
14 Sciences Humaines, Université Cadi Ayyad, rue Amarchich, Marrakech 40000, Morocco.

15 * Corresponding author; e-mail address: jean.david.moreau@gmail.com

16

17 **Abstract**

18 A new ichnofauna from the Permian of Morocco is described in details: it is the first
19 Palaeozoic ichnofauna from the Zat Valley in Marrakech High Atlas. The new tracksite was
20 found in the Tighdouine region, in the middle-upper Permian of the Cham-el-Houa Siltstone
21 Formation. An abundant and diverse ichnoassemblage composed of both protostomian
22 (probably arthropods and annelids) traces and vertebrate tracks is recorded. The presence of
23 protostomian burrows and traceways, associated with tetrapod tracks corresponds to the

24 *Scoyenia* ichnofacies. Protostomian traces are ascribed to *Diplichnites gouldi*, *Diplopodichnus*
25 *biformis*, *Scoyenia* cf. *gracilis* and *Spongiomorpha carlsbergi*. Tetrapod tracks include more
26 than 70 tracks attributed to *Amphisauropus*, *Erpetopus*, *Hyloidichnus*, *Characichnos*, and
27 indeterminate tracks. The co-occurrence of tetrapod tracks (both walking and swimming
28 tracks), protostomian traces, mudcracks, ripple marks, as well as the lithological features of
29 the track-bearing levels, indicate regularly inundated depositional environments during
30 periods of high discharge under a local seasonal climate. A sedimentological analysis shows
31 that the depositional environments evolved from braided-meandering systems to alluvial
32 floodplains. The track-bearing surfaces are mainly preserved in crevasse splays, levees and
33 pond deposits. This newly discovered ichnofauna helps to better reconstruct the
34 palaeoenvironments of the Marrakech High Atlas in Morocco during the Permian, and
35 enlarges the palaeogeographic distribution of important ichnotaxa.

36

37 **Keywords:** tetrapod tracks; protostomian traces; palaeoenvironment; Late Palaeozoic;
38 photogrammetry; Permian.

39

40 **1. Introduction**

41

42 Many studies demonstrated the fundamental role of tetrapod ichnofossils in the
43 reconstruction of Permian palaeofaunas and their interest in biostratigraphy (e.g. Voigt and
44 Lucas, 2018, but see Steyer, 2000 for biostratigraphy using bodyfossils). Many Permian
45 tracksites are located in Europe (e.g. Haubold and Sarjeant, 1973; Gand and Haubold, 1984;
46 Demathieu et al., 1992; Gand, 1993; Gand et al., 1997, 2000; Voigt, 2005; Gand and Durand,

47 2006; Voigt et al., 2012; Marchetti, 2016; Mujal et al., 2016; Marchetti et al., 2017a), Africa
48 (De Beer, 1986; Smith, 1993; de Klerk, 2002; Steyer et al., 2007; Smith et al., 2015;
49 Marchetti et al., 2019a), Asia (Gand et al., 2011), Australia (Warren, 1997), North America
50 (Mossman and Place, 1989; van Allen et al., 2005; Minter et al., 2007; Lucas et al., 2001,
51 2004; Marchetti et al., 2019b) and South America (Melchor and Sarjeant, 2004; da Silva et
52 al., 2012; Francischini et al., 2018).

53 In Morocco, the Permian deposits are broadly exposed in many graben structures forming
54 isolated basins (e.g. Broutin et al., 1998). Some of them yielded abundant and diverse tetrapod
55 bodyfossils (e.g., Dutuit, 1976, 1988; Jalil and Dutuit, 1996; Jalil, 1999; Jalil and Janvier,
56 2005; Germain 2010; Steyer and Jalil, 2009, Khaldoune et al., 2017). Permian tetrapod
57 tracksites are found in the Argana Basin (Voigt et al., 2010; Hminna et al., 2012), the
58 Khenifra Basin (Hmich et al., 2006; Voigt et al., 2011a) and the Tiddas Basin (Voigt et al.,
59 2011b). Recently, we discovered a new tracksite in the Cham-el-Houa Siltstone Formation
60 near Tighdouine, in the eastern-northeastern part of the Zat Valley in Marrakech High Atlas,
61 where Permian deposits are cropping out (Perez et al., 2019). It constitutes the first Permian
62 tracksite from this area. Here, we describe in details this new ichnoassemblage and its
63 sedimentological context in order to discuss the palaeoecosystem and palaeoenvironment of
64 the Cham-el-Houa Siltstone Formation.

65

66 **2. Geographical and geological setting**

67

68 The new tracksite is located in the Marrakech High Atlas (Fig. 1A), western side of
69 the Zat Valley; more precisely in the Tighdouine region, near the village of Al Bour (Fig. 1B
70 and 1C). This area is bounded by the Ourika-Zat Palaeozoic peri-anticline termination to the

71 SE and the Triassic strata to the NW. The occurrence of Carboniferous outcrops (Visean and
72 Stephanian) allows to examine post-Hercynian structures (Permian pre-rift) and their
73 relationships with older Hercynian structures, such as a NE-SW schistosity and fold axis. The
74 Hercynian overlaps are posterior to the schistosity. The Marrakech High Atlas contains
75 several Permian basins, which overly the deformed Variscan basement, represented mainly, in
76 the studied area, by Carboniferous mudstones. This basement is affected by the NNE-SSW to
77 NW-SE and E-W folds (Jenny, 1983; Cornée, 1989). The Atlasic orogeny consists of
78 Permian-Triassic to Early Jurassic distensional movement and Late Cretaceous compressive
79 movements. These Permian basins of the Marrakech High Atlas are described as pre-rift strata
80 (Olsen et al., 2000) and may be due to extensional tectonics (Perez et al., 2019).

81 The Permian basin of the Tighdouine area is composed of continental deposits that are
82 up to 160 m thick (Fig. 1). These deposits rest unconformably on Stephanian strata and are
83 unconformably covered by Triassic series (Fig. 1C). The western lateral equivalent of these
84 Tighdouine Permian strata corresponds to the Cham-el-Houa Siltstone Formation or F2
85 Formation *sensu* Biron (1982), identified in the Ourika and Gadji Valleys. The ichnofossils
86 described here were discovered *ex-situ* on large blocks lying in a Quaternary alluvial debris-
87 flow fan (Fig. 1C) but had come from a cliff composed of the Tighdouine Permian strata.

88

89 **3. Material and methods**

90

91 ***3.1. Sedimentological analysis***

92

93 The tracksite was discovered in 2018 during a palaeontological fieldtrip organised by
94 the MNHN (Paris, France) and the University Cadi Ayyad (Marrakech, Morocco) in the

95 Tighdouine region. In order to determine the stratigraphic origin of the tracks and to
96 characterise their depositional environments, a sedimentological analysis was conducted
97 along the 58-m-thick stratigraphic section accessible in the drainage basin of the Quaternary
98 fan (Figs. 1C and 2). The reconstruction of the depositional environment was established
99 through detailed facies and facies association analyses of the entire stratigraphic section.
100 Comparisons with facies of the *ex-situ* track-bearing blocks allowed to locate precisely the
101 track-bearing beds in the section (Fig. 2). The facies codes were completed according to Miall
102 (1978) and Postma (1990). The interpretation of depositional facies was based on analogous
103 modern dryland environments (Tooth, 2000a, b; Billi, 2007; North et al., 2007) and on facies
104 model of fluvial distributary systems (Nichols and Fisher, 2007; Fisher et al., 2007; Sáez et
105 al., 2007; Cain and Mountney, 2009; Burns et al., 2017, 2019; Gulliford et al., 2017).

106

107 **3.2. Ichnological analyses**

108

109 The palaeoichnological material from Tighdouine includes both protostomian
110 (probably arthropods and annelids) traces and tetrapod tracks. Tetrapod ichnofossils include
111 more than 70 tracks. They are preserved on five large *ex situ* isolated blocks found in the
112 debris-flow fan. The largest blocks (up to 2.2 m wide) bear four distinct palaeoichnological
113 assemblages labelled P.As-A to P.As-D. Assemblages A, B and D are preserved as convex
114 hyporeliefs (one block per assemblage) whereas Assemblage C includes convex hyporeliefs
115 as well as concave epireliefs and is preserved on two blocks. Additionally, numerous slabs
116 were collected: they are currently housed in the palaeontological collections of the Muséum
117 d'Histoire Naturelle de Marrakech, Morocco (hereafter MHNM). All blocks and slabs bearing
118 tracks consist of fine-grained reddish siltstone. The track-bearing surfaces often show
119 mudcracks forming large polygons (up to 60 cm wide), microbial mats, as well as ripple

120 marks. The descriptive terminology and biometric parameters used in this study follow
121 Haubold (1971) and Leonardi (1987). We used the following standard abbreviations: ML,
122 length of manus track; MW, width of manus track; ML/MW, length to width ratio of manus
123 track; PL., length of pes track; PW, width of pes track; and PL/PW, length to width ratio of
124 pes track. We use “L” for length and “W” for width when pes and manus tracks are
125 undifferentiated. 3D photogrammetric reconstructions (Mallison and Wings, 2014; Matthews
126 et al., 2016) were produced with the software Agisoft PhotoScan Professional 1.2.4. Pictures
127 of the surfaces were taken with a Nikon D5200 camera coupled with an AF-S Nikkor 18–105
128 mm f/3.5–5.6G ED lens. The same software was used to produce photogrammetric digital
129 elevation models and contours.

130

131 *3.3. Taxonomic nomenclature*

132

133 The name “Tetrapoda” refers to different taxa, according to the way these are
134 conceptualised. Traditionally in palaeontology, this name refers to an apomorphy-based taxon
135 defined by the occurrence of digitated limbs, or a suite of characters states including digitated
136 limbs. However, it is implicitly understood as a crown-clade taxon (i.e. excluding stem-
137 groups) in the bulk of the neontological nomenclature (Laurin and Anderson, 2004); thus, this
138 concept is explicitly formalised under the precepts of the PhyloCode (see Laurin, 2020 a; and
139 references therein). Concurrently, the name “Stegocephali” is formally defined to correspond
140 closely with the clade of limbed vertebrates (see Laurin, 2020 b; and reference therein). In
141 summary, the taxon encompassing all vertebrate taxa (extinct and extant) sharing digitated
142 limbs (including those who lost them) can be referred to either as “Tetrapoda” or
143 “Stegocephali”. To prevent confusion, and with regard to the adopted consensus in

144 palaeoichnology, we agreed to use the former, under its apomorphy-based concept. Rather
145 than using “invertebrate traces” we preferred “protostomian traces”, which is more accurate.

146

147 **4. Results**

148

149 ***4.1. Stratigraphy and sedimentology of the tracksite***

150

151 The new tracksite originates from the middle-upper section of the F2 Formation (Fig.
152 1C): this section is mainly characterised by fine-grained facies interbedded with silty and fine
153 sandy facies. The lower part of the section is more sandy than the upper part. The study of the
154 facies and facies associations allows to subdivide the section into three units (Fig. 2):

155 - Unit 1 (14.5 m thick) is characterised mainly by (1) sandstones and (2) heterolithic
156 beds. (1) The sandstones show rough trough-cross bedding (St facies), coarse planar-cross
157 bedding (Sp facies) to massive structure (Sm facies) and are topped by current ripple cross-
158 laminated sandstone (Sr facies), which is associated to *Scoyenia* burrows (Fig. 2). The facies
159 associations "St-Sr" and "Sm-Sp-Sr", both 8 m thick, characterise stacked channel deposits
160 (Fig. 2A) and are associated to *Scoyenia* burrows (Fig. 2B) at their top. (2) The heterolithic
161 beds, at the top of unit 1, are 3.5 m thick. They are dominated by massive and ripple cross-
162 laminated, up to 25 cm thick, fine sandstone beds (Sm and Sr facies) that coarsen and thicken,
163 and then fine upward (Fig. 2A). The subordinate cm- to dm-thick silty claystone layers
164 display a massive structure (Fm facies). The lateral accretion beds dip gently, on average, to
165 the west or to the east and evolve laterally into fine sediments. The upper part of the
166 heterolithic facies displays sometimes WNW-ESE axis scoured troughs, infilled with sets of
167 normally graded bedding (Fig. 2A). All these features reveal levee deposits.

168 - Unit 2 (28 m thick) shows four facies associations. (1) Medium to fine sandstone
169 beds are 1.5 to 3.0 m thick and 24 to 80 m wide. They are characterised by erosive base and
170 irregular top, with mainly massive (Sm facies) to subordinate rough trough-cross bedding (St
171 facies) and ripple cross-lamination (Sr facies) at their top. This facies association characterises
172 channel deposits. (2) Medium sandstone and siltstone beds are composed of planar cross
173 bedding (Sp facies) and ripple cross-lamination (Sr facies). The low-angle inclined lateral
174 accretion surfaces of beds are toward ENE or WSW, forming long belts of up to several
175 hundred meters. These surfaces isolate sigmoidal shape foresets (epsilon cross bedding). The
176 upper surface of sandstone bodies is irregular with ridges and swales topography (Fig. 2C).
177 The depositional environment was mid-point bars and upper point bars. (3) Heterolithic strata
178 are composed of massive or horizontally laminated very fine sandstones to siltstones (Sm, Sh
179 facies) and of fine-grained sediments. These latter are characterised by interlaminated
180 siltstone and claystones (Fl facies) or massive claystone (Fm facies) associated to mm-size
181 carbonate nodules and mottled fabric. This facies association sometimes shows a coarsening
182 and thickening upward trend. In transverse section, it includes WSW or ENE lateral accretion
183 (Fig. 2C). Plant macroremains (Fig. 2D), microbial mats (Fig. 2E) and some scoured troughs
184 are present. Plants consist of conifer leafy axes preserved as impressions without cuticles.
185 This facies association corresponds to levee deposits. (4) The wedge-shaped fine sandstones
186 to siltstones present horizontal bedding with E-W parting lineation (Sh facies) or ripple-cross
187 lamination (Sr facies) indicating a northward palaeocurrent. The longitudinal cross-section of
188 these sandy bodies (60 to 100 m long) documents their wing or wedge geometric relationship
189 with adjacent 10 to 40 m wide channels (Fig. 2F). The fourth facies association is interpreted
190 as crevasse splay deposits. Unit 2 is mainly characterised by heterolithically stratified
191 crevasse splay and levee deposits. All palaeocurrent measurements (from Sp/Sr facies, lateral
192 accretion, trough axis of erosion in levees and parting lineation) converge on the same

193 preferential SSE-NNW meandering channel palaeoflow direction, with WSW-ENE point bar
194 or levee lateral accretion and W-E to N expansion crevasse splay.

195 - Unit 3 (15.5 m thick) is characterised by mudstone interbedded with very fine-
196 grained sandstone to siltstone (Fig. 2G). (1) The fine-grained facies, up to 10 m thick, is
197 mainly massive (Fm facies) and associated with carbonate nodules and hydromorphic
198 palaeosols. This facies is sometimes bioturbated. (2) The thin sandy and silty beds are up to
199 50 cm thick and up to 80 m of lateral extent. They are mainly composed of climbing ripple
200 cross-lamination (Sr facies; Fig. 2H) and more rarely of horizontal lamination (Sh facies) and
201 present a massive structure (Sm facies). These facies associations characterise distal crevasse
202 splays. The palaeocurrents are directed toward the north. The unit 3 facies associations are
203 typical of distal floodplain deposits that evolve locally to ponds, as attested by swimming
204 tetrapod tracks, small wave ripples, syneresis cracks (Fig. 2I) and microbial mats (Fig. 2E).

205

206 ***4.2. Systematic palaeoichnology***

207

208 ***4.2.1. Traces of protostomians***

209

210 *Diplichnites* Dawson, 1873

211 *Diplichnites gouldi* Gevers et al., 1971

212 Fig. 3A–B

213 *Material.* MHNM.ZAT.01, slab with three traceways preserved as convex hyporeliefs.

214 MHNM.ZAT.14a, slab with one traceway preserved as convex hyporeliefs. MHNM.ZAT.18,

215 slab with several traceways preserved as convex hyporeliefs.

216 *Description.* Traceways are simple, straight to curved and consist of two parallel rows of
217 numerous and elongated appendage imprints that are regularly arranged and commonly
218 oriented perpendicular to the traceway midline but can be inclined at up to 65°. Traceways are
219 up to 13 cm long. External traceway width is 6–14 mm, whereas internal traceway width is 2–
220 6 mm. Traces of appendages are closely spaced, consecutive imprints being separated by a
221 distance of up to 2.5 mm. Traces of appendages are up to 3 mm long, up to 2 mm wide and
222 sometimes show a bifid end.

223 *Remarks.* As suggested by Minter et al. (2007), the taxonomy of *Diplichnites* and close
224 relatives (e.g. *Acripes*, *Asaphoidichnus*, *Lineatichnus*, *Merostomichnites*, *Multipodichnus*,
225 *Pentapodichnus*, *Petalichnus*, *Protichnites*, *Tasmanadia*, *Trachomatichnus* and *Umfolozia*)
226 needs to be revised. Although the oldest report of *Diplichnites gouldi* is Ordovician in age
227 (Buatois et al., 1998; Retallack, 2009) the ichnospecies was reported from several Permian
228 tracksites throughout the world (e.g. Minter et al., 2007; Avanzini et al., 2011a; Lucas et al.,
229 2011; Marchetti et al., 2015).

230

231 *Diplopodichnus* Brady, 1947

232 *Diplopodichnus biformis* Brady, 1947

233 Fig. 3C–D

234 *Material.* MHNM.ZAT.01 and MHNM.ZAT.15, slabs including several traceways preserved
235 as convex hyporeliefs.

236 *Description.* The slab MHNM.ZAT.01 bears several traceways, occasionally crossing and
237 running in different directions. The longest traceway is of 82 mm. Traceways are horizontal,

238 unbranched, straight to winding, and up to 2.5 mm wide. They consist of two thin and up to 1
239 mm wide parallel hypichnial ridges separated by a central groove that is up to 0.5 mm wide.

240 *Remarks.* The ichnogenus *Diplopodichnus* is reported from the Upper Proterozoic to the
241 Lower Jurassic (Buatois et al., 1998; Uchman et al., 2011 and references therein). *D. biformis*
242 is widely recorded in Palaeozoic deposits including many occurrences in Permian formations
243 worldwide (e.g. Brady, 1947; Lucas et al., 2004, 2005; Contardi and Santi, 2009; Avanzini et
244 al., 2011a; Lima and Netto, 2012).

245

246 *Scoyenia* White, 1929

247 *Scoyenia* cf. *gracilis* White, 1929

248 Fig. 3E–F

249 *Material.* Several burrows on P.As-C.

250 *Description.* Burrows are unbranched, horizontally to vertically oriented in the sedimentary
251 layer, straight to slightly curved, with prominently meniscate back-filled by the circular in
252 cross-section and up to 20 mm in diameter.

253 *Remarks.* The specimens are preserved in cross section; longitudinal ridges commonly
254 observed on the surface of the burrow are not visible. *Scoyenia* is commonly observed in non-
255 marine formations yielding vertebrate trackways. In Morocco, this ichnotaxon was previously
256 reported from several vertebrate tracksites of diverse Permian basins (e.g. Argana Basin,
257 Hminna et al., 2012; Khenifra Basin, Hmich et al., 2006; Tiddas Basin, Voigt et al., 2011b).

258

259 *Spongeliomorpha* Saporta, 1887

260 *Spongeliomorpha carlsbergi* (Bromley & Asgaard, 1979)

261 Fig. 3G–H

262 *Material.* MHNM.ZAT.01 and MHNM.ZAT.15, slabs with several burrows preserved as
263 convex hyporeliefs.

264 *Description.* Burrows are convex, mainly horizontally oriented in the sedimentary layer,
265 sometimes oblique, cylindrical in cross section, irregularly curved. They are randomly
266 arranged, simple to ramified, sometimes exhibiting a Y- or T-bifurcation. The longest
267 specimen is of 60 mm. Burrows are 2–4 mm in diameter. The outer surface of the burrows
268 shows a striate texture. Striae are very thin, up to 2 mm long, and obliquely to transversally
269 oriented to the main axes of the burrow. Striae consist of convex ridges.

270 *Remarks.* The morphology of *Spongeliomorpha* is similar to those of *Steinichnus* (Bromley
271 and Asgaard, 1979). Both consist of burrow networks with striated walls having dominantly
272 transverse to oblique striae. The burrows from the Tighdouine tracksite are similar to the
273 ichnospecies *Steinichnus carlsbergi* (Bromley and Asgaard, 1979) and *Spongeliomorpha*
274 *milfordensis* (Metz, 1993), which have only been recorded in nonmarine settings (Melchor et
275 al., 2009). Melchor et al. (2009) transferred *Steinichnus carlsbergi* to *Spongeliomorpha*
276 *carlsbergi* and considered the ichnospecies *S. milfordensis* as a junior synonym of
277 *Spongeliomorpha carlsbergi*, based on a similar range of orientation of striae. This report
278 consists of the second occurrence of *Spongeliomorpha carlsbergi* in the Permian of Morocco.
279 The ichnospecies was described from the middle to upper Permian Ikakerm Formation of the
280 Argana Basin (Hminna et al., 2012).

281

282 **4.2.2. Tracks of tetrapods**

283

284 *Amphisauropus* Haubold, 1970

285 *Amphisauropus* isp.

286 Fig. 4

287 *Material.* MHN.M.ZAT.02, slab with four tracks preserved as convex hyporeliefs.

288 *Description.* The tracks consist of two plantigrade to semi plantigrade pes/manus sets (Fig.
289 4A–B). Pes and manus strides are 60 mm long. Pes and manus tracks from the same set form
290 a divergent angle of 30–35°. Pes imprints are pentadactyl, nearly as long as wide (; PL=4.0
291 cm, PW=4.0–4.4 cm; Fig. 4). The PL/PW ratio is equal to 0.9. Digit imprints are quite short,
292 straight to curved and end in a small enlarged rounded tip. Digits I to V show a sub-parallel
293 arrangement. Digit impressions increase in length from I to IV. Pes tracks show a short, large,
294 rectangular sole with a fairly straight proximal margin (Fig. 4). Manus imprints are almost
295 symmetrical, pentadactyl, and smaller than the pes tracks. They are twice as wide as long
296 (ML=1.8 cm; MW=3.7–3.8 cm; ML/MW= 0.5; Fig. 4). Imprints of digits are very short and
297 end in a small enlarged rounded tip. The traces of digit V is poorly imprinted or absent. The
298 divarication angle of digits I-IV is equal to 90°.

299 *Remarks.* Although these tracks share some similarities with *Dolomitipes*, this ichnogenus
300 differs in showing pedal imprint of similar size or slightly smaller than the manus, digit
301 impressions I–IV length about 1/3 of the pes length, and manual imprint about one third wider
302 than long (Marchetti et al. 2019a). Although these tracks share some features with
303 *Merifontichnus*, this ichnogenus differs in showing manus and pes tracks with similar size and
304 morphology, pes tracks clearly wider than long, and digits I–IV radially disposed (Gand et al.,
305 2000; Marchetti, 2016). Frequently reported in the Lower Permian (e.g. Lucas et al., 2001;
306 Santi and Krieger, 2001; van Allen et al., 2005; Avanzini et al., 2011b; Voigt et al., 2012),

307 *Amphisauropus* is also present in the upper Permian (Melchor and Sarjeant, 2004; Ptaszyński
308 and Niedźwiedzki, 2004; Hminna et al., 2012). *Amphisauropus* was described from many
309 countries: in Argentina (Melchor and Sarjeant, 2004); Canada (Mossman and Place, 1989;
310 van Allen et al., 2005); France (e.g. Gand and Haubold, 1984; Gand, 1987); Germany
311 (Haubold, 1971; Voigt, 2005); Italy (e.g. Santi and Krieger, 2001; Avanzini et al., 2008,
312 2011b; Marchetti, 2016; Marchetti et al., 2013a, 2013b, 2015); Poland (Ptaszyński and
313 Niedźwiedzki, 2004; Voigt et al., 2012) and USA (Lucas et al., 2001). In Africa, the
314 ichnogenus was previously reported from Morocco, in the lower Permian of the Tiddas Basin
315 (Voigt et al., 2011b) and in the middle to upper Permian Ikakerm Formation of the Argana
316 Basin (Hminna et al., 2012).

317

318 *Erpetopus* Moodie, 1929

319 *Erpetopus* isp.

320 Fig. 5

321 *Material.* Thirty tracks. Thirteen preserved as convex hyporeliefs on P.As-A, fifteen as
322 concave epireliefs on MHN.M.ZAT.03, and two as convex hyporeliefs on MHN.M.ZAT.05.

323 *Description.* The tracks are small, plantigrade and consist of several isolated pes/manus sets
324 and two trackways. The longest trackway (on P.As-A) is 53 cm whereas the better preserved
325 one (MHN.M.ZAT.03) is 16.0 cm long and 4.6 cm wide (Fig. 5A–B). Pes and manus track
326 stride is 3.8–4.9 cm long. The pes tracks are oriented inward, forming an acute angle of up to
327 30° with the trackway axis. The manus tracks are oriented forward, parallel with the trackway
328 axis.

329 Pes imprints are pentadactyl, as long as wide or slightly longer than wide, 9–15 mm long and
330 8–15 mm wide (Fig. 5C–I). The PL/PW ratio varies from 1.0 to 1.2. Digit imprints are thin,

331 elongated, curved and show sharp claw traces. Imprints of digits I-IV are curved inward
332 whereas imprint of digit V is curved outward. The divarication angle of digits I-V varies from
333 55 to 100°. Pes tracks show a well-imprinted, rectangular and longer than wide sole (Fig. 5C–
334 I).

335 Manus imprints are pentadactyl and smaller than pes tracks, wider than long or as wide as
336 long (ML=5–8 mm, MW=6–12 mm; Fig. 5J–K). The ML/MW ratio varies from 0.7 to 1.2.
337 Digit imprints are thin, elongated and distally curved. The impression of the digit IV is the
338 longest. The divarication angle of digits I-V varies from 120 to 180°. Manus tracks show a
339 very short sole (Fig. 5J–K). The manus tracks are commonly shallower than the pes tracks or
340 entirely absent.

341 *Remarks.* Although these tracks share some similarities with *Procolophonichnium*, this
342 ichnotaxon differs in showing manus and pes of similar shape, and manus slightly longer than
343 wide (Marchetti et al, 2019c). The ichnogenus *Rhynchosauroides* differs from our tracks by
344 the presence of digitigrade pes tracks, and a larger size of the tracks (Voigt and Lucas, 2018).
345 *Erpetopus* was previously reported from lower and upper Permian deposits of many areas
346 including France (Haubold and Lucas 2003), Italy (Haubold and Lucas 2003; Marchetti et al.,
347 2013a, 2015) and USA (Minter et al., 2007; Marchetti et al., 2019b). In Africa, the
348 ichnogenus was only previously reported from the middle to upper Permian Ikakerm
349 Formation of the Argana Basin, Morocco (Hminna et al., 2012).

350

351 *Hyloidichnus* Gilmore, 1927

352 *Hyloidichnus* isp.

353 Fig. 6

354 *Material.* Eight tracks; six preserved as concave epireliefs on MHNM.ZAT.11, and two as
355 convex hyporeliefs on P.As-D.

356 *Description.* Tracks are semi-plantigrade, pentadactyl, wider than long or as long (L=3.3–4.9
357 cm) as wide (W=4.0–5.0 cm; Fig. 6A–D). The L/W ratio varies from 0.7 to 1.1. Digit imprints
358 are elongated, straight and end in a small enlarged rounded, sometimes bifurcated tip. The
359 impression of digit IV is the longest. The digit V is weakly impressed. Digits I–V have a
360 divarication angle of 82 to 95°. Tracks sometimes show a short sole with a straight to slightly
361 concave proximal margin (Fig. 6C–D).

362 *Remarks.* *Hyloidichnus* was reported from lower and upper Permian deposits of many
363 localities throughout the world, in Argentina (Melchor and Sarjeant, 2004); France (e.g. Gand
364 and Haubold, 1984; Gand, 1987; Demathieu et al., 1992; Gand and Durand, 2006); Italy (e.g.
365 Marchetti et al., 2013b, 2015; Marchetti, 2016); Spain (Gand et al., 1997; Mujal et al., 2016);
366 Turkey (Gand et al., 2011); and USA (Lucas et al., 2012; Voigt and Lucas, 2015, 2017). In
367 Niger, possible *Hyloidichnus* trackways were reported from the ?middle to upper Permian
368 (Steyer et al., 2007). In Morocco, the ichnogenus was previously reported from the middle to
369 upper Permian Ikakerm Formation in the Argana Basin, Morocco (Voigt et al., 2010; Hminna
370 et al., 2012).

371

372 *Characichnos* Whyte & Romano, 2001

373 *Characichnos* isp.

374 Fig. 7

375 *Material.* Sixteen tracks. Six tracks preserved as both concave epireliefs and convex
376 hyporeliefs on P.As-C. MHNM.ZAT.07 slab with a single track preserved as concave

377 epirelief. MHNM.ZAT.08 slab with seven further tracks preserved as concave epireliefs and
378 MHNM.ZAT.09 slab with two tracks shown as concave epireliefs.

379 *Description.* The six tracks on P.As-C form a 81 cm long trackway. Tracks follow a 24.5–30
380 cm long stride (Fig. 7A). Outer and inner widths of trackway are 23 cm and 15 cm,
381 respectively. Tracks are more or less parallel to the trackway axis. Morphology and
382 dimensions of individual tracks vary a lot along the trackway: this is the case for example of
383 the length (L=17–70 mm) and the width (W=18–38 mm) of the tracks. Tracks show two to
384 four parallel, elongated, thin and straight to curved furrows of uniform width (Fig. 7B–M).
385 Some of the tracks show probable claw traces.

386 *Remarks.* The stratigraphic range of *Characichnos* is very large; from the lower Permian to
387 the Cretaceous (Whyte and Romano, 2001). This ichnogenus is reported from Permian
388 localities throughout the world (e.g. Argentina, Melchor and Sarjeant, 2004; Spain, Mujal et
389 al., 2016; USA, Lucas and Spielmann, 2009, Lerner and Lucas, 2015). Such tracks were
390 interpreted by several authors as scratches produced by the backward motion of the digits by a
391 partially buoyant tetrapod in shallow water (Whyte and Romano, 2001; Melchor and Sarjeant,
392 2004). Here, only the tips of the digits touched the substrate.

393

394 Undetermined tracks

395

396 Morphotype A

397 Fig. 8

398 *Material.* Five tracks preserved as convex hyporeliefs on P.As-B.

399 *Description.* P.As-B (Fig. 8A–B) includes a single pes/manus set (Fig. 8C–D). Pes imprints
400 are semi-plantigrade, pentadactyl, and twice as wide (PW=5.0–5.4 cm) as long (PL=2.4–2.9;
401 Fig. 8E–F). The PL/PW ratio is equal to 0.5. Digit imprints are very short, straight and end in
402 an enlarged rounded tip. Digit V seems to be the shortest of the series, weakly impressed or
403 lacking. The divarication angle of digits I–V is 121°. Pes tracks show a short, large and
404 weakly impressed sole (Fig. 8E–F). Manus imprints are tetradactyl and almost as long
405 (ML=4.9 cm) as wide (MW=4.6 cm; Fig. 8C–D). Digit imprints are short, straight and end in
406 an enlarged rounded tip. Imprints of digits increase in length from I to IV. The divarication
407 angle of digits I–IV is 120°.

408 *Remarks.* On manus tracks, impression of digit IV being the longest suggests that impression
409 of digit V is missing. Although tracks of Morphotype A share some similarities with
410 *Dolomitipes*, this ichnotaxon differs in showing pedal imprint longer than wide or about as
411 wide as long, of similar size or slightly smaller than the manus (Marchetti et al. 2019a).
412 Tracks of the Morphotype A also share some similarities with *Capitosauroides*. However, this
413 ichnotaxon differs from Morphotype A in showing as long as wide pes tracks with relatively
414 longer digits than those of manus tracks (Marchetti et al., 2019c). Given the partial
415 preservation of these tracks, we refrain from assigning this material to an ichnogenus.

416

417 Morphotype B

418 Fig. 9

419 *Material.* Six tracks preserved as convex hyporeliefs on P.As-D.

420 *Description.* The tracks consist of plantigrade pes/manus sets (Fig. 9A–C). Pes imprints are
421 pentadactyl and longer than wide (PL= 5.0–7.8 cm; PW= 3.2–5.3 cm; PL/PW=1.3–1.6; Fig.

422 9A–C). The PL/PW ratio varies from 1.3–1.6. Digit imprints are mainly straight and only
423 occasionally curved. The length of digits increases from I to IV. The divarication angle of
424 digits I–V is up to 65°. A long heel impression is longer than half of the total length of the pes
425 tracks. Manus imprints are tetradactyl, smaller than pes tracks, wider than long or as long
426 (ML=3.7–5.0 cm) as wide (MW=2.8–3.7 cm) (Fig. 9A–C). The ML/MW ratio varies from 1.0
427 to 1.7. Digit imprints are curved to straight and end by an enlarged rounded tip. Digits
428 increase in length from I to III.

429 *Remarks.* Morphotype B differs from Morphotype A by the presence of a long heel
430 impression on pes tracks. It also differs by digit impressions which are not all straight
431 (particularly on manus imprints) and not distally rounded (particularly on pes imprints). The
432 presence of tetradactyl manus imprints is characteristic of the ichnogenera *Batrachichnus* and
433 *Limnopus*. However, *Batrachichnus* is smaller than Morphotype B and in both ichnogenera
434 *Batrachichnus* and *Limnopus*, impressions of digits are commonly distally rounded (Voigt
435 and Lucas, 2018). Although tracks of the Morphotype B share some similarities with
436 *Dolomitipes*, this ichnotaxon differs in showing pedal imprint of similar size or slightly
437 smaller than the manus (Marchetti et al. 2019a).

438

439 **5. Discussion**

440

441 **5.1. Age of the tracksite**

442

443 The age of the red beds of the Anrar Conglomerate Formation (F1) and the Cham-el-
444 Houa Siltstone Formation (F2) from the Ourika-Zat anticline has been debated in the past

445 (Van-Houten, 1977; Biron, 1982). Due to the poorness of biostratigraphic data, these
446 formations were tentatively dated from the upper Carboniferous to the Lias (see Biron, 1982
447 and references therein). Based on correlations with volcanic layers from neighbouring basins,
448 Biron (1982) proposed that the formations F1 and F2 are lower Permian in age. However,
449 Perez et al. (2019) recently performed Pb/U datations of the formations F1 and F2 based only
450 on two samples (one by formation) they collected in the south-western part of the Ourika-Zat
451 anticline, about 20 km west from the tracksite described here: in the sample from the F1, they
452 identified high proportions of 250-270 Ma and 271-331 Ma zircons, the youngest being of
453 247.8 ± 7.2 Ma, with a peak at around 264 Ma (=Capitanian according to the ICC, i.e. middle
454 Permian). In the sample from the F2, they identified five zircons of 260-270 Ma, the youngest
455 being of 266.3 ± 3.9 Ma (=Wordian according to the ICC, i.e. middle Permian). Although
456 some zircons from the F2 are artefactually older than those from the underlying F1, the
457 calculated ages of both F1 and F2 are mostly from the middle Permian, possibly upper
458 Permian for the youngest zircons. This fits with the comparable middle to upper Permian age
459 given to the Ikakern Formation (T1 and T2 units) of the Argana Basin. The ichnoassemblage
460 reported by Hminna et al. (2012) from the upper member of the Ikakern Formation shares
461 strong similarities with those we described here from the F2 Formation of the Zat Valley (co-
462 occurrence of *Amphisauropus*, *Erpetopus*, *Dromopus*, *Scoyenia* and *Spongeliomorpha*).

463

464 ***5.2. Tracemakers and their palaeoenvironments***

465

466 The ichnoassemblage suggests that the fauna from Tighdouine was composed of
467 various protostomians, especially arthropods. *Diplichnites gouldi*, *Scoyenia cf. gracilis* and
468 *Spongeliomorpha carlsbergi* are characteristic of non-marine palaeoenvironments.

469 *Diplichnites* is usually attributed to a locomotion trace of multi-limb arthropods such as
470 crustaceans, myriapods, and euthycarcinoids (Minter et al., 2007). *Scoyenia* is interpreted as a
471 feeding or a combined feeding and locomotion trace (burrow), produced by arthropods or
472 annelids (Bromley and Asgaard, 1979; Frey et al., 1984). *Spongiomorpha carlsbergi* is
473 commonly interpreted as traces produced by burrowing insects (Melchor et al., 2009). The
474 ichnospecies *Diplopodichnus biformis* was reported from non-marine to marginal marine
475 environments and currently attributed to diplopods or other myriapods (Buatois et al., 1998).

476 The tetrapod tracks suggest that the fauna from Tighdouine was mainly composed of
477 amniotes, and more specifically, reptiles. Only *Amphisauropus*, whose trackmakers are
478 supposed to be seymouriamorphs (Haubold, 2000; Marchetti et al., 2017b), may correspond to
479 anamniotic tetrapods. Trackmakers of *Erpetopus* are interpreted as small captorhinids or
480 protorhothyridids (Haubold and Lucas, 2003; Bernardi and Avanzini, 2011). *Hyloidichnus* are
481 usually referred to basal captorhinids (Gand, 1987) or possibly Moradisaurinae (Voigt et al.,
482 2010). These supposed trackmakers (basal captorhinids, Moradisaurinae) are highlighted by
483 bone remains in the contemporary Argana Basin (see Khaldoune et al., 2017 for a review).

484 The presence of protostomian burrows and traceways with tetrapod tracks matches the
485 *Scoyenia* ichnofacies, which are interpreted as subaqueous freshwater sediments that are
486 periodically emerged or as terrestrial substrates that are frequently inundated (Buatois and
487 Mángano, 1995; Buatois et al., 1997). The co-occurrence of tetrapod tracks (both walking and
488 swimming tracks), continental protostomian traces, mudcracks, ripple marks, as well as the
489 lithological features of the track-bearing levels, confirm that the depositional environment
490 was a fluvial zone periodically flooded and emerged. The presence of plant macro-remains
491 indicates the relative proximity to forests or overgrown riverbanks. The depositional
492 environments of the middle to upper part of the F2 Formation, around the tracksite, are
493 characterised by a retrogradational trend. It evolves from fluvial deposits with stacked

494 channels of distal braided system (Unit 1) to meandering river, which records interstratified
495 point bars / levees and channel depositional facies (Unit 2). The upper part (Unit 3) of this
496 sedimentary evolution is marked by a distal floodplain, showing distal crevasse splays
497 associated with local ponds. The studied tetrapod trackways are located in crevasse splays,
498 levees and pond deposits.

499

500 **6. Conclusion**

501

502 New ichnofossils from Tighdouine (Zat Valley) were discovered *ex-situ* in Permian
503 blocks lying in a Quaternary alluvial debris-flow fan. These trace-bearing blocks come from
504 the Cham-el-Houa Siltstone Formation or F2 *sensu* Biron (1982). A detailed sedimentological
505 analysis confirms their stratigraphic origin: the new traces are considered to belong to the
506 middle-upper Permian. They constitute the first report of a Palaeozoic ichnoassemblage in the
507 Marrakech High Atlas and provide crucial information for the reconstruction of Permian
508 ecosystems of Morocco. Protostomians traces (*Diplichnites gouldi*, *Diplopodichnus biformis*,
509 *Scoyenia cf. gracilis* and *Spongiomorpha carlsbergi*) are mainly attributed to diverse
510 arthropods as well as possible annelids. The tetrapod tracks (*Amphisauropus*, *Characichnos*,
511 *Erpetopus* and *Hyloidichnus*) suggest that the fauna from Tighdouine was mainly composed
512 of sauropsid amniotes. The sedimentological analysis shows that this fauna lived in a
513 palaeoenvironment evolving from braided-meandering systems to distal floodplains.

514

515 **Acknowledgements**

516 We thank Matteo Belvedere and Eudald Mujal for their constructive and thoughtful reviews
517 on the manuscript. We thank Georges Gand (University of Burgundy, Dijon, France) and El
518 Hassane El Arabi (University of Hassan II, Casablanca, Morocco) for helpful discussions and
519 references. J-D M was supported by the CNRS-UMR 6538 Laboratoire Géosciences Océan,
520 Université Bretagne Sud, France. Fieldwork was supported by the European program Geopark
521 H2020 Rise. For authorization to work in the Zat Valley, we warmly thank Mr. A.
522 Benlakhdim, from Morocco's Department of Energy and Mines, Ministry of Energy, Mines
523 and sustainable development.

524

525 **References**

- 526 Avanzini, M., Neri, C., Nicosia, U., Conti, M.A., 2008. A new early Permian ichnocoenosis
527 from the “Gruppo vulcanico atesino” (Mt. Luco, Southern Alps, Italy). *Studi Trent. Sci.*
528 *Nat., Acta Geol.* 83, 231–236.
- 529 Avanzini, M., Contardi, P., Ronchi, A., Santi, G., 2011a. Ichnosystematics of the lower
530 Permian invertebrate traces from the Collio and Mt. Luco Basins (North
531 Italy). *Ichnos* 18, 95–113.
- 532 Avanzini, M., Bernardi, M., Nicosia, U., 2011b. The Permo-Triassic tetrapod faunal diversity
533 in the Italian southern Alps. *Earth and Environmental Sciences*. Intech Open Access,
534 591–608. Doi: 10.5772/27233
- 535 Beauchamp, J., 1988. Triassic sedimentation and rifting in the High Atlas (Morocco). *Dev.*
536 *Geotectonics* 22, 477–497.

- 537 Benaouiss, N., Courel, L., Beauchamp, J., 1996. Rift-controlled fluvial/tidal transitional series
538 in the Oukaïmeden Sandstones, High Atlas of Marrakesh (Morocco). *Sediment. Geol.*
539 107, 21–36.
- 540 Bernardi, M., Avanzini, M., 2011. Locomotor behavior in early reptiles: insights from an
541 unusual *Erpetopus* trackway. *J. Paleontol.* 85, 925–929.
- 542 Billi, P., 2007. Morphology and sediment dynamics of ephemeral stream terminal distributary
543 systems in the Kobo Basin (northern Welo, Ethiopia). *Geomorphology* 85, 98–113.
- 544 Biron, P., 1982. Le Permo-Trias de la région de l'Ourika (Haut Atlas de Marrakech, Maroc).
545 Unpublished PhD diss. Université de Grenoble, France.
- 546 Brady, L.F., 1947. Invertebrate tracks from the Coconino Sandstone of northern Arizona. *J.*
547 *Paleontol.* 21, 466–472.
- 548 Bromley, R., Asgaard, U., 1979. Triassic freshwater ichnocoenoses from Carlsberg Fjord, east
549 Greenland. *Palaeogeogr. Palaeoclimatol. Palaeoecol.* 28, 39–80.
- 550 Broutin, J., Aassoumi, H., El Wartiti, M., Freytet, P., Kerp, H., Quesada, C., Toutin-Morin,
551 N., 1998. The Permian basins of Tiddas, Bou Achouch and Khenifra (central Morocco).
552 Biostratigraphic and palaeophytogeographic implications. *Mém. Mus. Nat. Hist.*
553 *Nat.* 179, 257–278.
- 554 Buatois, L.A., Mángano, M.G., 1995. The paleoenvironmental and paleoecological
555 significance of the lacustrine *Mermia* ichnofacies: an archetypical subaqueous
556 nonmarine trace fossil assemblage. *Ichnos* 4, 151–161.
- 557 Buatois, L.A., Mángano, M.G., Maples, C.G., 1997. The paradox of nonmarine ichnofaunas
558 in tidal rhythmites; integrating sedimentologic and ichnologic data from the Late
559 Cretaceous of eastern Kansas, USA. *Palaios* 12, 467–481.

- 560 Buatois, L.A., Mángano, M.G., Maples, C.G., Lanier, W.P., 1998. Taxonomic reassessment of
561 the ichnogenus *Beaconichnus* and additional examples from the Carboniferous of
562 Kansas, USA. *Ichnos* 5, 287–302.
- 563 Burns, C.E., Mountney, N.P., Hodgson, D.M., Colombera, L., 2017. Anatomy and
564 dimensions of fluvial crevasse-splay deposits: examples from the Cretaceous Castlegate
565 Sandstone and Neslen Formation, Utah, USA. *Sediment. Geol.* 351, 21–35.
- 566 Burns, C.E., Mountney, N.P., Hodgson, D.M., Colombera, L., 2019. Stratigraphic architecture
567 and hierarchy of fluvial overbank splay deposits. *J. Geol. Soc.* 176, 629–649.
- 568 Cain, S.A., Mountney, N.P., 2009. Spatial and temporal evolution of terminal fan system: the
569 Permian Organ Rock Formation, South-east Utah, USA. *Sedimentology* 56, 1774–1800.
- 570 Contardi, P., Santi, G., 2009. New observations on the invertebrate ichnofossils of the Lower
571 Permian basins from Southern Alps (Northern Italy). *Rev. Paléobiol.* 28, 333–347.
- 572 Cornée, J.-J., 1989. Le Haut Atlas occidental paléozoïque : un reflet de l’histoire hercynienne
573 du Maroc occidental, stratigraphie, sédimentologie et tectonique. Unpublished PhD diss.
574 Université de Marseille, France.
- 575 Da Silva, R.C., Sedor, F.A., Fernandes, A.C.S., 2012. Fossil footprints from the Late Permian
576 of Brazil: an example of hidden biodiversity. *J. S. Am. Earth Sci.* 38, 31–43.
- 577 De Beer, C.H., 1986. Surface markings, reptilian footprints and trace fossils on a paleosurface
578 in the Beaufort Group near Fraserburg, C. P. *Ann. Geol. Opname* 20, 129–140.
- 579 De Klerk, W.J., 2002. A dicynodont trackway from the *Cistecephalus* assemblage zone in the
580 Karoo, east of Graaff-Reinet, South Africa. *Palaeont. Afr.* 38, 73–91.

581 Demathieu, G., Gand, G., Toutin-Morin, N., 1992. La palichnofaune des bassins permien
582 provençaux. *Geobios* 25, 19–54.

583 Dutuit, J.-M., 1976. Il est probable que les Rhynchocéphales sont représentés dans la faune du
584 Trias marocain. *C.R. Acad. Sci. Paris* 283, 483–486.

585 Dutuit, J.-M., 1988. *Diplocaulus minimus* n. sp. (Amphibia: Nectridea), Lépospondyle de la
586 formation d’Argana dans l’Atlas occidental marocain. *C.R. Acad. Sci. Paris* 307, 851–
587 854.

588 Fisher, J.A., Nichols, G.J., Waltham, D.A., 2007. Unconfined flow deposits in distal sectors
589 of fluvial distributary systems: examples from the Miocene Luna and Huesca Systems,
590 northern Spain. *Sed. Geol.* 195, 55–73.

591 Francischini, H., Dentzien-Dias, P., Lucas, S.G., Schultz, C.L., 2018. Tetrapod tracks in
592 Permo–Triassic eolian beds of southern Brazil (Paraná Basin). *PeerJ* 6: e4764; DOI
593 10.7717/peerj.4764.

594 Frey, R.W., Pemberton, S.G., Fagerstrom, J.A., 1984. Morphological, ethological, and
595 environmental significance of the ichnogenera *Scoyenia* and *Ancorichnus*. *J. Paleontol.*
596 58, 511–528.

597 Gand, G., 1987. Les traces de vertébrés tétrapodes du Permien français (paléontologie,
598 stratigraphie, paléoenvironnements). Unpublished PhD diss. Université de Dijon,
599 France.

600 Gand, G., 1993. La palichnofaune de vertébrés tétrapodes du bassin permien de Saint-
601 Affrique (Aveyron) : comparaisons et conséquences stratigraphiques. *Géol. de la*
602 *France* 1, 41–56.

603 Gand, G., Haubold, H., 1984. Traces de vertébrés du Permien du Bassin de Saint-Affrique
604 (Description, datation, comparaison avec celle du bassin de Lodève). Géol.
605 Méditerr. 11, 321–351.

606 Gand, G., Durand, M., 2006. Tetrapod footprint ichno-associations from French Permian
607 basins. Comparisons with other Euramerican ichnofaunas. Geol. Soc. Spe. Publ. 265,
608 157–177.

609 Gand, G., Kerp, H., Parsons, C., Martínez-García, E., 1997. Paleoenvironmental and
610 stratigraphic aspects of animal traces and plant remains in Spanish Permian red beds
611 (Pena Sagra, Cantabrian Mountains, Spain). Geobios 30, 295–318.

612 Gand, G., Garric, J., Demathieu, G., Ellenberger, P., 2000. La palichnofaune de vertébrés
613 tétrapodes du Permien supérieur du bassin de Lodève (Languedoc-France).
614 Palaeovertebrata 29, 1–52.

615 Gand, G., Tüysüz, O., Steyer, J.-S., Allain, R., Sakiñç, M., Sanchez, S., Şengör, A.M.C., Sen,
616 S., 2011. New Permian tetrapod footprints and macroflora from Turkey (Çakraz
617 Formation, northwestern Anatolia): biostratigraphic and palaeoenvironmental
618 implications. CR Palevol 10, 617–625.

619 Germain, D., 2010. The Moroccan diplocaulid: the last lepospondyl, the single one on
620 Gondwana. Hist. Biol. 22, 4–39.

621 Gulliford, A.R., Flint, S.S., Hodgson, D.M., 2017. Crevasse splay processes and deposits in
622 an ancient distributive fluvial system: the lower Beaufort Group, South Africa.
623 Sediment. Geol. 358, 1–18.

624 Haubold, H., 1971. Ichnia amphibiorum et reptiliorum fossilium. Handbuch der
625 Paläoherpetologie 18, 1–124.

- 626 Haubold, H., 2000, Tetrapodenfährten aus dem Perm - Kenntnisstand und Progress 2000:
627 Hallesches Jahrb. Geowiss. B 22,1–16.
- 628 Haubold, H., Lucas, S.G., 2003. Tetrapod footprints of the lower Permian Choza formation at
629 Castle Peak, Texas. *Paläontol. Z.* 77, 247–261.
- 630 Haubold, H., Sarjeant, W.A.S., 1973. Tetrapodenfährten aus den Keele und Enville Groups
631 (Permokarbon: Stefan und Autun) von Shropshire und South Staffordshire,
632 Großbritannien. *Z. Geol. Wiss.* 1, 895–933.
- 633
- 634 Hmich, D., Schneider, J.W., Saber, H., Voigt, S., El Wartiti, M., 2006. New continental
635 Carboniferous and Permian faunas of Morocco: implications for biostratigraphy,
636 palaeobiogeography and palaeoclimate. *Geol. Soc. Spe. Pub.* 265, 297–324.
- 637 Hminna, A., Voigt, S., Saber, H., Schneider, J.W., Hmich, D., 2012. On a moderately diverse
638 continental ichnofauna from the Permian Ikakern Formation (Argana Basin, Western
639 High Atlas, Morocco). *J. African Earth Sci.* 68, 15–23.
- 640 Jalil, N.-E., 1999. Continental Permian and Triassic vertebrate localities from Algeria and
641 Morocco and their stratigraphical correlations. *J. African Earth Sci.* 29, 219–226.
- 642 Jalil, N.-E., Dutuit, J.-M., 1996. Permian captorhinid reptiles from the Argana formation,
643 Morocco. *Palaeontology* 39, 907–918.
- 644 Jalil, N.-E., Janvier, P., 2005. Les pareiasaures (Amniota, Parareptilia) du Permien supérieur
645 du Bassin d’Argana, Maroc. *Geodiversitas* 27, 35–132.
- 646 Jenny, J., 1983. Zone de décrochement du Tizi-n-Test dans le Haut Atlas. *Eclogae Geol. Helv.*
647 76, 249–251.
- 648 Khaldoune F., Jalil N.-E., Germain G., Steyer J.-S., 2017. Les vertébrés du Permien et du
649 Trias du Maroc (Bassin d’Argana, Haut Atlas occidental) : fenêtre ouverte sur

650 l'évolution autour de la grande crise fini-paléozoïque. Mém. de la Soc. Géol. France
651 180, 103–168.

652 Leonardi, G., 1987. Glossary and manual of tetrapod footprint palaeoichnology. Ministerio
653 Minas Energie, Departamento Nacional da Producao Mineral, Brasilia.

654 Lagnaoui, A., Voigt, S., Saber, H., Schneider, J.W., 2014. First occurrence of tetrapod
655 footprints from Westphalian strata of the Sidi Kassem Basin, central
656 Morocco. *Ichnos* 21, 223–233.

657 Laurin, M., 2020 a. *Tetrapoda*. In: Cantino, P.D., de Queiroz, K., Gauthier, J.A. (Eds.), pp.
658 759-764. *Phylonyms: An Implementation of PhyloCode*. CRC Press, Boca Raton,
659 Florida.

660 Laurin, M., 2020 b. *Stegocephali*. In: Cantino, P.D., de Queiroz, K., Gauthier, J.A. (Eds.), pp.
661 741-745. *Phylonyms: An Implementation of PhyloCode*. CRC Press, Boca Raton,
662 Florida.

663 Laurin, M., Anderson, J.S., 2004. Meaning of the name Tetrapoda in the scientific literature:
664 an exchange. *Syst. Biol.* 53, 68–80.

665 Laville, E., Piqué, A., 1991. La distension crustale atlantique et atlasique au Maroc au début
666 du Mésozoïque : le jeu des structures hercyniennes. *Bull. Soc. Géol. Fr.* 162, 1161–
667 1171.

668 Lerner, A.J., Lucas, S.G., 2015. A *Selenichnites* ichnoassociation from the early Permian tidal
669 flats of the Prehistoric Trackways National Monument of south-central New Mexico. In:
670 Lucas, S. G., DiMichele, W. A. (Eds.). *Carboniferous-Permian Transition in the*
671 *Robledo Mountains, Southern New Mexico*. *Bull. New Mexico Mus. Nat. Hist. Sci.* 65,
672 141–152.

673 Lima, J.H.D., Netto, R.G., 2012. Trace fossils from the Permian Teresina Formation at Cerro
674 Caveiras (S Brazil). *Rev. Bras. Paleontolog.* 15, 5–22.

675 Lucas, S.G., 2007. Tetrapod footprint biostratigraphy and biochronology. *Ichnos* 14, 5–38.

676 Lucas, S.G., Spielmann, J.A., 2009. Tetrapod footprints from the Lower Permian Abo
677 Formation near Bingham, Socorro County, New Mexico. *New Mexico Geol. Soc.*
678 *Guidebook* 60, 299–304.

679 Lucas, S.G., Lerner, A.J., Haubold, H., 2001. First record of *Amphisauropus* and *Varanopus*
680 in the Lower Permian Abo Formation, central New Mexico. *Hallesches Jahrb. Geowiss.*
681 *B* 23, 69–78.

682 Lucas, S.G., Lerner, A.J., Hunt, A.P., 2004. Permian tetrapod footprints from the Lucero
683 uplift, central New Mexico, and Permian footprint biostratigraphy. *Bull. New Mexico*
684 *Mus. Nat. Hist. Sci.* 25, 291–300.

685 Lucas, S.G., Smith, J.A., Hunt, A.P., 2005. Tetrapod tracks from the Lower Permian Yeso
686 Group, central New Mexico. *Bull. New Mexico Mus. Nat. Hist. Sci.* 31, 121–124.

687 Lucas, S.G., Voigt, S., Lerner, A.J., Nelson, W.J., 2011. Late early Permian continental
688 ichnofauna from Lake Kemp, north-central Texas, USA. *Palaeogeogr. Palaeoclimatol.*
689 *Palaeoecol.* 308, 395–404.

690 Lucas, S.G., Krainer, K., Chaney, D.S., DiMichele, W.A., Voigt, S., Berman, D.S., Henrici,
691 A.C., 2012. The Lower Permian Abo Formation in the Fra Cristobal and Caballo
692 mountains, Sierra County, New Mexico. *New Mexico Geol. Soc. Guidebook* 63, 345–
693 376.

694 Mallison, H., Wings O., 2014. Photogrammetry in paleontology – a practical guide. J.
695 Paleontol. Techn. 12, 1–31.

696 Marchetti, L., 2016. New occurrences of tetrapod ichnotaxa from the Permian Orobic Basin
697 (Northern Italy) and critical discussion of the age of the ichnoassociation. Pap.
698 Palaeontol. 2, 363–386.

699 Marchetti, L., Bernardi, M., Avanzini, M., 2013a. Some insights on well-preserved
700 *Amphisauropus* and *Erpetopus* trackways from the Eastern Collio basin (Trentino-Alto
701 Adige, NE Italy). B. Soc. Paleontol. Ital. 52, 55–62.

702 Marchetti, L., Avanzini, M., Conti, M.A., 2013b. *Hyloidichnus bifurcatus* Gilmore, 1927 and
703 *Limnopus heterodactylus* (King, 1845) from the Early Permian of Southern Alps (N
704 Italy): a new equilibrium in the ichnofauna. Ichnos 20, 202–217.

705 Marchetti, L., Ronchi, A., Santi, G., Voigt, S., 2015. The Gerola Valley site (Orobic Basin,
706 Northern Italy): a key for understanding late Early Permian tetrapod
707 ichnofaunas. Palaeogeogr. Palaeoclimatol. Palaeoecol. 439, 97–116.

708 Marchetti, L., Tessarollo, A., Felletti, F., Ronchi, A., 2017a. Tetrapod footprint paleoecology:
709 behavior, taphonomy and ichnofauna disentangled. A case study from the Lower
710 Permian of the Southern Alps (Italy). Palaios 32, 506–527.

711 Marchetti, L., Mujal, E., Bernardi, M., 2017b. An unusual *Amphisauropus* trackway and its
712 implication for understanding seymouriamorph locomotion. Lethaia 50, 162–174.

713 Marchetti, L., Klein, H., Buchwitz, M., Ronchi, A., Smith, R.M.H., De Klerk, W.J., Sciscio
714 L., Groenewald, G.H., 2019a. Permian-Triassic vertebrate footprints from South Africa:
715 Ichnotaxonomy, producers and biostratigraphy through two major faunal crises.
716 Gondwana Res. 72, 139–168.

- 717 Marchetti, L., Voigt, S., Lucas, S.G., Francischini, H., Dentzien-Dias, P., Sacchi, R.,
718 Mangiacotti, M., Scali, S., Gazzola, A., Ronchi, A., Millhouse, A., 2019b. Tetrapod
719 ichnotaxonomy in eolian paleoenvironments (Coconino and De Chelly formations,
720 Arizona) and late Cisuralian (Permian) sauropsid radiation. *Earth-Sci. Rev.* 190, 148–
721 170.
- 722 Marchetti, L., Voigt, S., Klein, H., 2019c. Revision of Late Permian tetrapod tracks from the
723 Dolomites (Trentino-Alto Adige, Italy). *Hist. Biol.* 31, 748–783.
- 724 Matthews, N., Noble, T., Breithupt, B.H., 2016. Close-Range photogrammetry for 3D
725 ichnology: the basics of photogrammetric ichnology. In: Falkingham, P.L., Marty, D.,
726 Richter, A. (Eds.), *Dinosaur Tracks—The next steps*. Indiana University Press,
727 Bloomington and Indianapolis.
- 728 Melchor, R.N., Sarjeant, W.A.S., 2004. Small amphibian and reptile footprints from the
729 Permian Carapacha Basin, Argentina. *Ichnos* 11, 57–78.
- 730 Melchor, R.N., Bromley, R.G., Bedatou, E., 2009. *Spongeliomorpha* in nonmarine settings:
731 an ichnotaxonomic approach. *Earth Env. Sci. Tr. R. Soc.* 100, 429–436.
- 732 Metz, R., 1993. A new ichnospecies of *Spongeliomorpha* from the Late Triassic of New
733 Jersey. *Ichnos* 2, 259–62.
- 734 Miall, A.D., 1978. Lithofacies types and vertical profile models in braided river deposits: a
735 summary. In: Miall, A.D. (Ed.), *Fluvial Sedimentology*. Can Soc. Petrol. Geol. Mem. 5,
736 597–604.
- 737 Minter, N.J., Krainer, K., Lucas, S.G., Braddy, S.J., Hunt, A.P., 2007. Palaeoecology of an
738 Early Permian playa lake trace fossil assemblage from Castle Peak, Texas,
739 USA. *Palaeogeogr. Palaeoclimatol. Palaeoecol.* 246, 390–423.

740 Mossman, D. J., Place, C.H., 1989. Early Permian fossil vertebrate footprints and their
741 stratigraphic setting in megacyclic sequence II red beds, Prim Point, Prince Edward
742 Island. *Can. J. Earth Sci.* 26, 591–605.

743 Mujal, E., Fortuny, J., Oms, O., Bolet, A., Galobart, À., Anadón, P., 2016.
744 Palaeoenvironmental reconstruction and early Permian ichnoassemblage from the NE
745 Iberian Peninsula (Pyrenean Basin). *Geol. Mag.* 153, 578–600.

746 Nichols, G.J., Fisher, J.A., 2007. Processes, facies and architecture of fluvial distributary
747 system deposits. *Sed. Geol.* 195, 75–90.

748 North, C.P., Nanson, G.C., Fagan, S.D., 2007. Recognition of the sedimentary architecture of
749 dryland anabranching (anastomising) rivers. *J. Sed. Res.* 77, 925–938.

750 Olsen, P.E., Kent, D.V., Fowell, S.J., Schlische, R.W., Withjack, M.O., LeTourneau, P.M.,
751 2000. Implications of a comparison of the stratigraphy and depositional environments of
752 the Argana (Morocco) and Fundy (Nova Scotia, Canada) Permian-Jurassic basins. In
753 Oujidi, M., Et-Touhami, M. (Eds.). *Le Permien et le Trias du Maroc, Actes de la*
754 *Première Réunion du Groupe Marocain du Permien et du Trias*, 165–183.

755 Perez, N.D., Teixell, A., Gómez-Gras, D., Stockli, D.F., 2019. Reconstructing extensional
756 basin architecture and provenance in the Marrakech High Atlas of Morocco:
757 implications for rift basins and inversion tectonics. *Tectonics* 38, 1584–1608.

758 Postma, G., 1990. Depositional architecture and facies of river and fan deltas: a synthesis. In:
759 Colella, A., David, B.P. (Eds.). *Coarse-grained deltas. Int. Assoc. Sedimentol. Spe. Pub.*
760 10, 13–28.

761 Ptaszyński, T. & Niedźwiedzki, G., 2004. Late Permian vertebrate tracks from the Tumlin
762 Sandstone, Holy Cross Mountains, Poland. *Acta Palaeontol. Pol.* 49, 289–320.

- 763 Retallack, G. J. (2009). Cambrian–Ordovician non-marine fossils from South
764 Australia. *Alcheringa* 33, 355–391.
- 765 Sáez, A., Anadón, P., Herrero, M.J., Moscariello, A., 2007. Variable style of transition
766 between Palaeogene fluvial fan and lacustrine systems, southern Pyrenean foreland, NE
767 Spain. *Sedimentology* 54, 367–390.
- 768 Santi, G., Krieger, C., 2001. Lower Permian tetrapod footprints from Brembana Valley-
769 Orobic Basin (Lombardy, Northern Italy). *Rev. Paléobiol.* 20, 45–68.
- 770 Smith, R.M., 1993. Sedimentology and ichnology of floodplain paleosurfaces in the Beaufort
771 Group (Late Permian), Karoo sequence, South Africa. *Palaios* 8, 339–357.
- 772 Smith, R.M., Sidor, C.A., Tabor, N.J., Steyer, J.-S., 2015. Sedimentology and vertebrate
773 taphonomy of the Moradi Formation of northern Niger: a Permian wet desert in the
774 tropics of Pangaea. *Palaeogeogr. Palaeoclimatol. Palaeoecol.* 440, 128–141.
- 775 Steyer, J.-S., 2000. Are European Paleozoic amphibians good stratigraphical markers? *Bull.*
776 *Soc. Géol. France* 171, 127–135.
- 777 Steyer, J.-S., Gand, G., Smith, R., Sidor, C., Tabor, N., 2007. The first tetrapod trackways
778 from the Paleozoic of West Africa: one step towards reconstructing the landscape of
779 central Pangea. *J. Vertrebr. Paleontol.* 27, 152A.
- 780 Steyer, J.-S., Jalil, N.-E., 2009. First evidence of a temnospondyl in the Late Permian of the
781 Argana Basin, Morocco. *Spec. Pap. Palaeontol.* 81, 155–160.
- 782 Tooth, S., 2000a. Downstream changes in dryland river channels: the Northern Plains of arid
783 central Australia. *Geomorphology* 34, 33–54.
- 784 Tooth, S., 2000b. Process, form and change in dryland rivers: a review of recent research.
785 *Earth-Sci. Rev.* 51, 67–107.

- 786 Uchman, A., Hu, B., Wang, Y., Song, H., 2011. The trace fossil *Diplopodichnus* from the
787 Lower Jurassic lacustrine sediments of central China and the isopod *Armadillidium*
788 *vulgare* (Pillbug) lebensspuren as its recent analogue. *Ichnos* 18, 147–155.
- 789 Van Allen, H.E., Calder, J.H., Hunt, A.P., 2005. The trackway record of a tetrapod
790 community in a walchian conifer forest from the Permo-Carboniferous of Nova
791 Scotia. *Bull. New Mexico Mus. Nat. Hist. Sci.* 30, 322–332.
- 792 Van Houten, F.B., 1977. Triassic-Liassic deposits of Morocco and Eastern North America:
793 comparison. *Am. Assoc. Pet. Geol. Bull.* 61, 79–99.
- 794 Voigt, S., 2005. Die Tetrapodenichnofauna des kontinentalen Oberkarbon und Perm im
795 Thüringen Wald: Ichnotaxonomie, Paläoökologie und Biostratigraphie. Cuvillier
796 Verlag, Göttingen.
- 797 Voigt, S., Lucas, S.G., 2015. Permian tetrapod ichnodiversity of the Prehistoric Trackways
798 National Monument (south-central New Mexico, USA). *Bull. New Mexico Mus. Nat.*
799 *Hist. Sci.* 65, 153–167.
- 800 Voigt, S., Lucas, S.G., 2018. Outline of a Permian tetrapod footprint ichnostratigraphy. *Geol.*
801 *Soc. Spe. Publ.* 450, 387–404.
- 802 Voigt, S., Lucas, S.G., 2017. Early Permian tetrapod footprints from central New Mexico. In:
803 Lucas, S. G., DiMichele, W. A., Krainer, K. (Eds.). Carboniferous-Permian transition in
804 Socorro County, New Mexico. *Bull. New Mexico Mus. Nat. Hist. Sci.* 77, 333–352.
- 805 Voigt, S., Hminna, A., Saber, H., Schneider, J.W., Klein, H., 2010. Tetrapod footprints from
806 the uppermost level of the Permian Ikakern Formation (Argana Basin, western High
807 Atlas, Morocco). *J. African Earth Sci.* 57, 470–478.

808 Voigt, S., Saber, H., Schneider, J.W., Hmich, D., Hminna, A., 2011a. Late Carboniferous-
809 Early Permian tetrapod ichnofauna from the Khenifra Basin, central
810 Morocco. *Geobios* 44, 399–407.

811 Voigt, S., Lagnaoui, A., Hminna, A., Saber, H., Schneider, J.W., 2011b. Revisional notes on
812 the Permian tetrapod ichnofauna from the Tiddas Basin, central Morocco. *Palaeogeogr.*
813 *Palaeoclimatol. Palaeoecol.* 302, 474–483.

814 Voigt, S., Niedźwiedzki, G., Raczyński, P., Mastalerz, K., Ptaszyński, T., 2012. Early
815 Permian tetrapod ichnofauna from the Intra-Sudetic basin, SW Poland. *Palaeogeogr.*
816 *Palaeoclimatol. Palaeoecol.* 313, 173–180.

817 Warren, A., 1997. A tetrapod fauna from the Permian of the Sydney Basin. *Rec. Aust. Mus.*
818 49, 25–33.

819 Whyte, M.A., Romano, M., 2001. A dinosaur ichnocoenosis from the Middle Jurassic of
820 Yorkshire, UK. *Ichnos* 8, 223–234.

821 Woodworth, J.B., 1900. Vertebrate footprints on Carboniferous shales of Plainville,
822 Massachusetts. *Geol. Soc. Am. Bull.* 11, 449–454.

823
824
825
826
827
828
829
830
831

832 **Figure captions**

833

834 **Figure 1.** Location in space (A-B) and time (C) of the new tracksite. A, Permo-Triassic
835 outcrops in northern Morocco (modified after Beauchamp, 1988; Laville and Piqué, 1991).
836 The rectangular frame indicates the central region of the Marrakech High Atlas. WHA:
837 Western High Atlas; MHA: Marrakech High Atlas; CHA: Central High Atlas; EHA: Eastern
838 High Atlas; MA: Middle Atlas. B, Permian and Triassic outcrops in Marrakech High Atlas
839 (compiled by Benaouiss, in Benaouiss et al., 1996). The rectangular frame indicates the
840 location of the Tighdouine region. C, Geological sketch map of the western bank of the Zat
841 Valley (modified from Google Earth and personal data of N.B. and A.T.) showing the
842 location of the tracksite (star) and the studied sedimentological section. The synthetic
843 lithostratigraphic log of the study area represents the legend of C.

844

845 **Figure 2.** Detailed sedimentary section and outcrop photographs of the middle to upper part
846 of the Permian F2 Formation in the western bank of the Zat Valley. The stratigraphic position
847 of the ichnofossils is indicated by symbols. A, Stacked channels (CH) superimposed by levee
848 architectural element (Lv), with progradational and retrogradational trend. The erosional
849 event appears at the top as infilled trough with graded beds (dashed line). B, *Scoyenia*
850 burrows (Sc) at the top of channels, common in the lower and upper parts of the section. C,
851 Juxtaposed point bars (Pb) of the unit 2 lower part, showing ridges and swales topography in
852 their upper surface. Levee beds (Lv) with lateral accretion to the left indicated by white
853 dashed lines. D, Conifer leafy axes mainly found in levee depositional facies. E, Crinkled
854 surface (Cr) of microbial mats observed in levee, crevasse splay and pond deposits, associated
855 with syneresis cracks (Sy). F, Outcrop aspect of channel bodies (CH) and lateral wing

856 crevasse splays (Cp) interbedded with heterolithic facies crevasse splay/levee (Cp/Lv). G,
857 Outcrop of unit 3 upper part with silty distal crevasse splay (Cp) in distal floodplain. H,
858 Climbing ripples in crevasse splay. I, mm-size syneresis cracks in pond deposits of unit 3.

859

860 **Figure 3.** Protostomian traces. A–B, *Diplichnites gouldi*; photograph (A) and interpretative
861 sketch (B). C–D, *Diplopodichnus biformis*; photograph (C) and interpretative sketch (D). E–F,
862 *Scoyenia cf. gracilis*; photograph (E) and interpretative sketch (F). G–H, *Spongeliomorpha*
863 *carlsbergi*; photograph (G) and interpretative sketch (H). A–D, G–H: MHNM.ZAT.01; E–F:
864 P.As-C. Scale bars: A–F = 1 cm; G–H = 2 mm.

865

866 **Figure 4.** *Amphisauropus* isp. A–B, Siltstone slab bearing two successive pes/manus sets
867 preserved as convex hyporeliefs; photograph (A) and interpretative sketch (B). C–D,
868 Pes/manus set; photograph (C) and interpretative sketch (D). MHNM.ZAT.02. All scale bars
869 = 1 cm.

870

871 **Figure 5.** *Erpetopus* isp. A–B, trackway showing several pes/manus sets. A–I, pes tracks;
872 photographs (C, E, G), interpretative sketches (D, F, H) and digital elevation models in false
873 colors (I). J–K, manus tracks; photographs (J) and interpretative sketch (K). A–D, J–K:
874 MHNM.ZAT.03; E–H: P.As-A. Scale bars: A–I = 1 cm; J–K = 0.5 cm.

875

876 **Figure 6.** *Hyloidichnus* isp. A–B, Siltstone slab bearing several tracks; photograph (A) and
877 interpretative sketch (B). C–D, Detail of tracks; photograph (C) and interpretative sketch (D).
878 Scale bars: A–B = 2 cm.

879

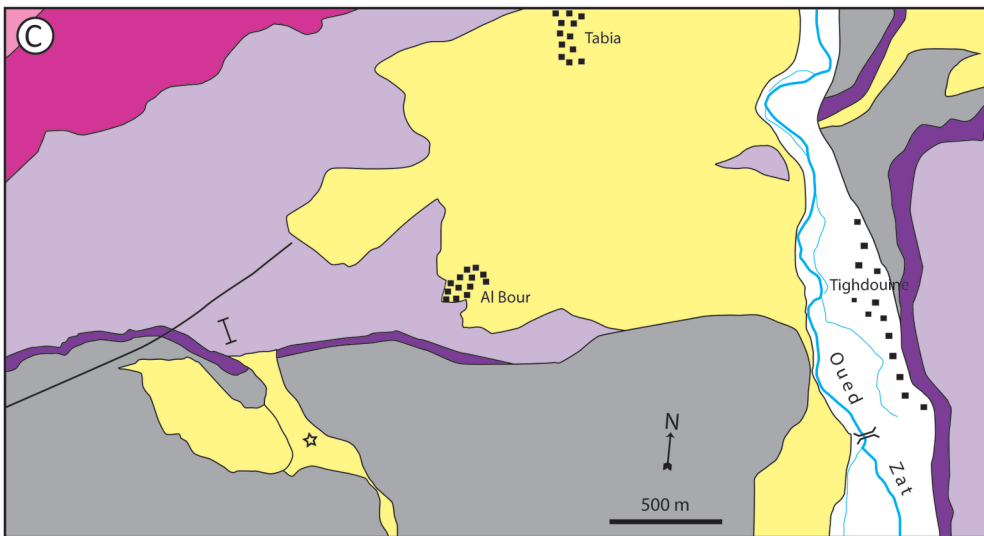
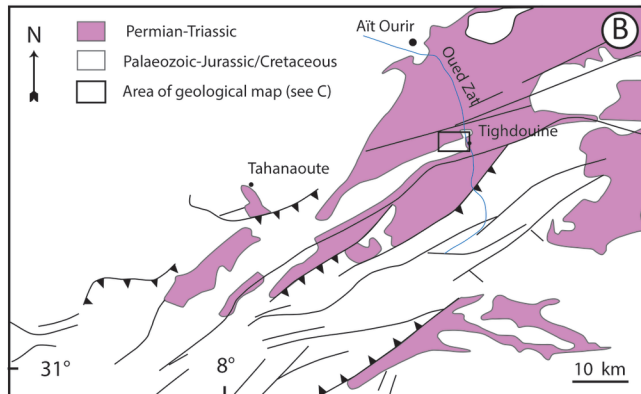
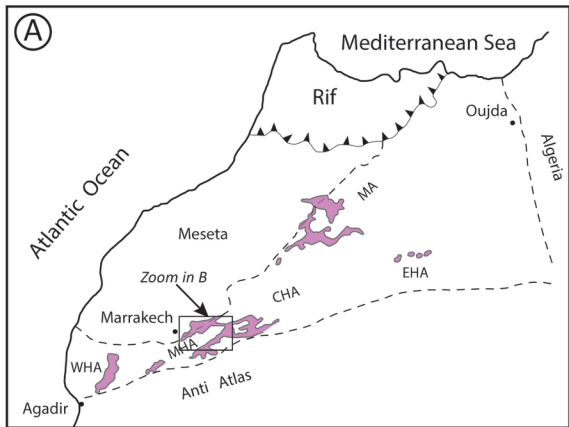
880 **Figure 7.** *Characichnos* isp. A, trackway consisting of six tracks; interpretative sketch. B–G,
881 diverse siltstone slabs bearing isolated tracks; photographs (B, D, F) and interpretative
882 sketches (C, E, G). H–M, detail of tracks showing up to four parallel, elongated, thin, and
883 curved furrows; photographs (H, J, L) and digital elevation models in false colors (I, K, M).
884 A, J–M: P.As-C; B–C: MHN.M.ZAT.08; D–E: MHN.M.ZAT.09; F–I: MHN.M.ZAT.07. Scale
885 bars: A = 10 cm; B–M = 2 cm.

886

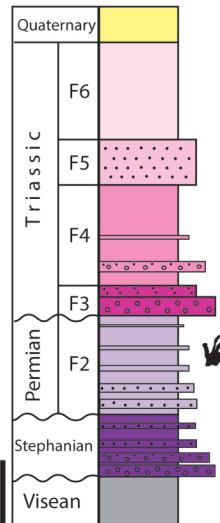
887 **Figure 8.** Morphotype A. A–B, Surface of the slab P.As-B showing several tracks preserved
888 as convex hyporeliefs; photograph (A) and interpretative sketch (B). C–D, Pes/manus set;
889 photograph (C) and interpretative sketch (D). Pes track; photographs (E) and digital elevation
890 models in false colors and contours (F). Scale bars: A–B = 10 cm; C–F = 1 cm.

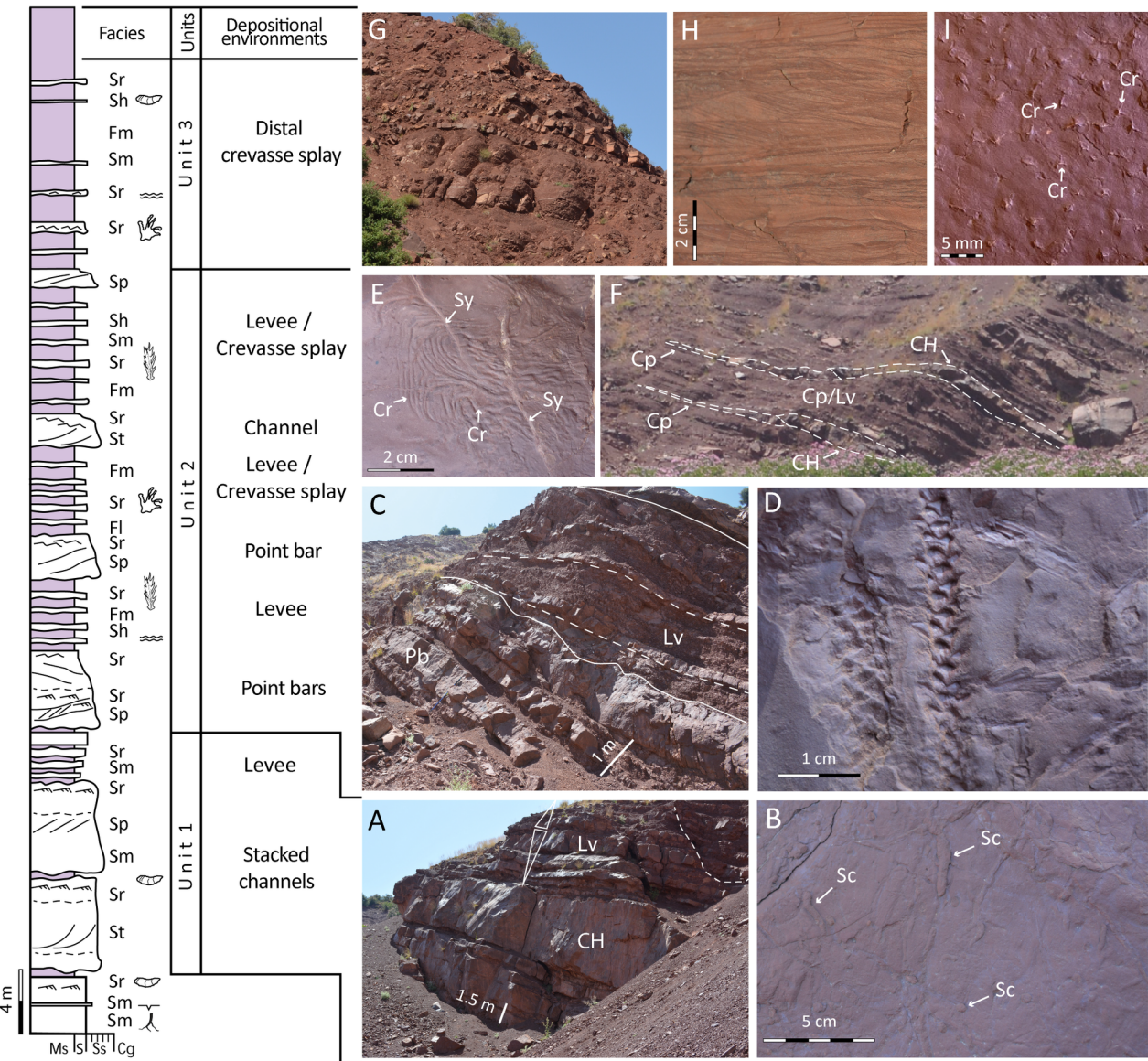
891


892 **Figure 9.** Morphotype B. Pes/manus set preserved as convex hyporeliefs on P.As-D;
893 photograph (A), digital elevation model in false colors and contours (B) and interpretative
894 sketch (C). Scale bars: A–C = 1 cm.




Legend of C








Rootlets 

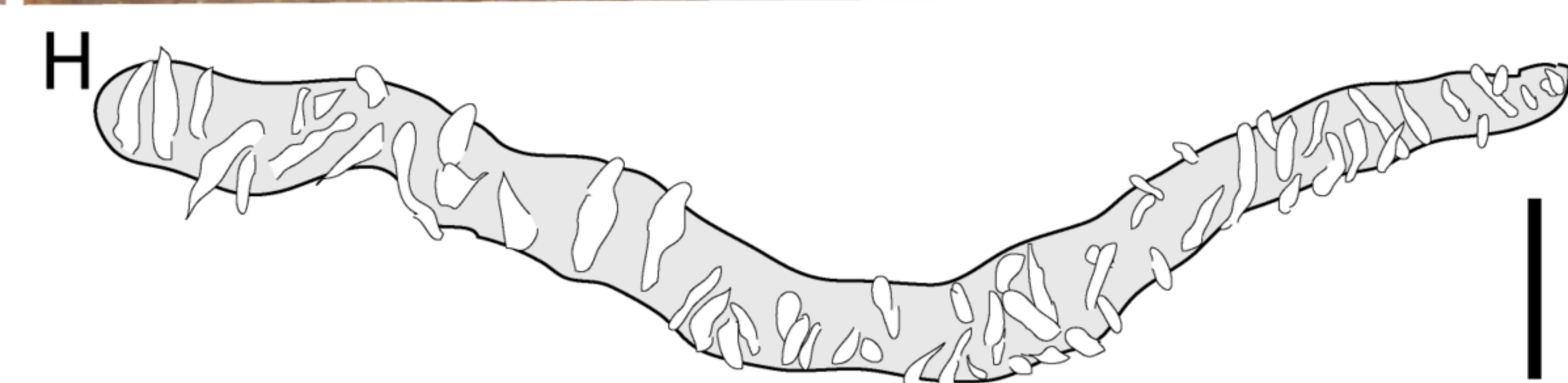
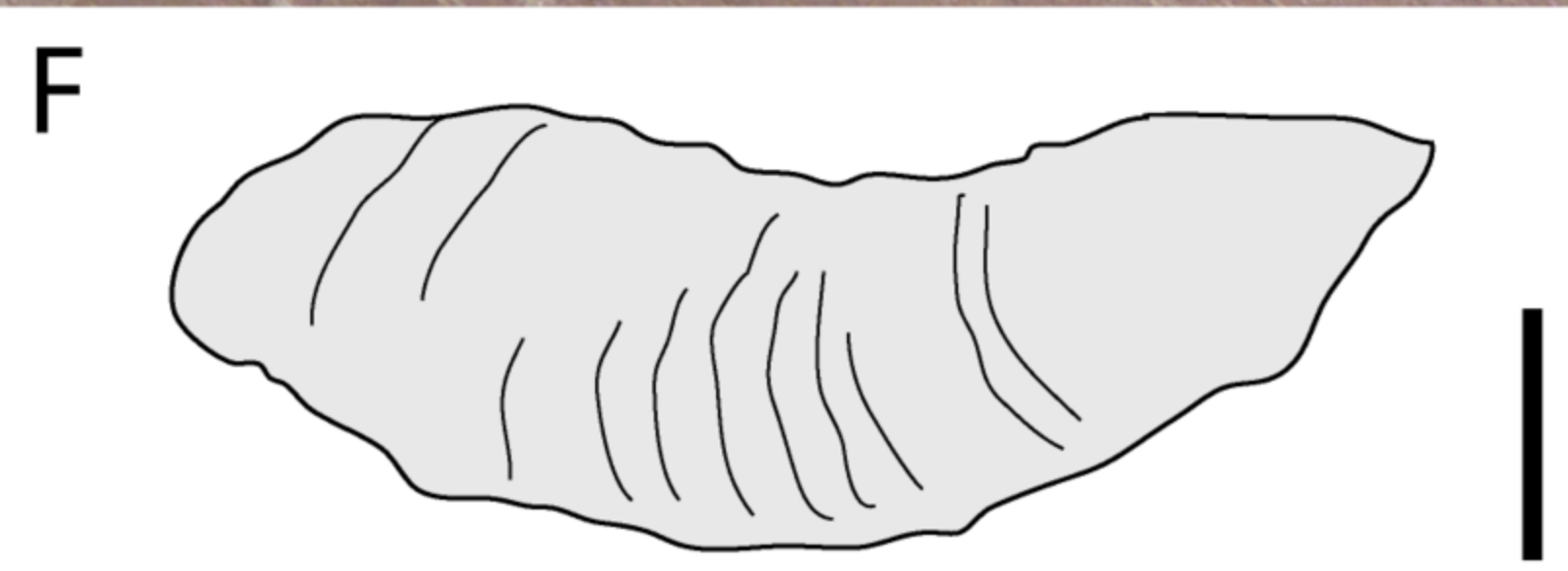
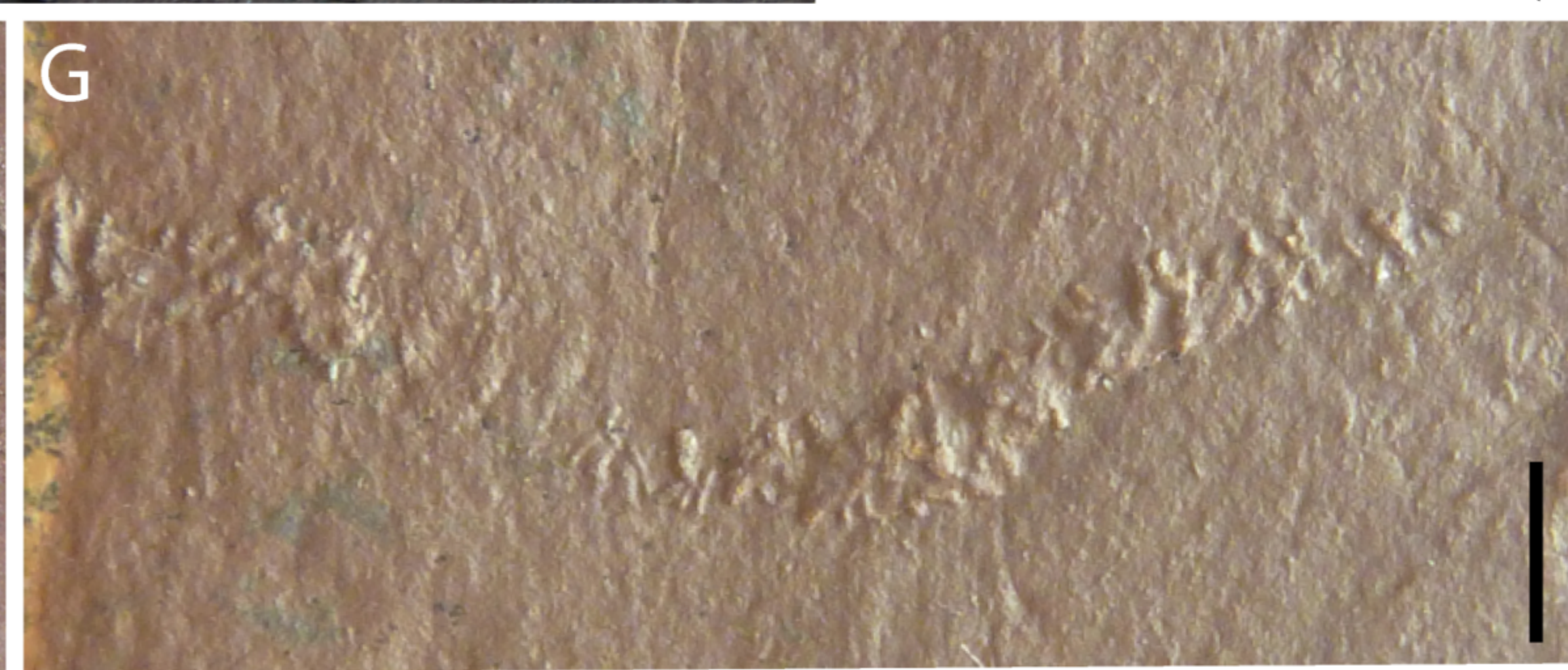
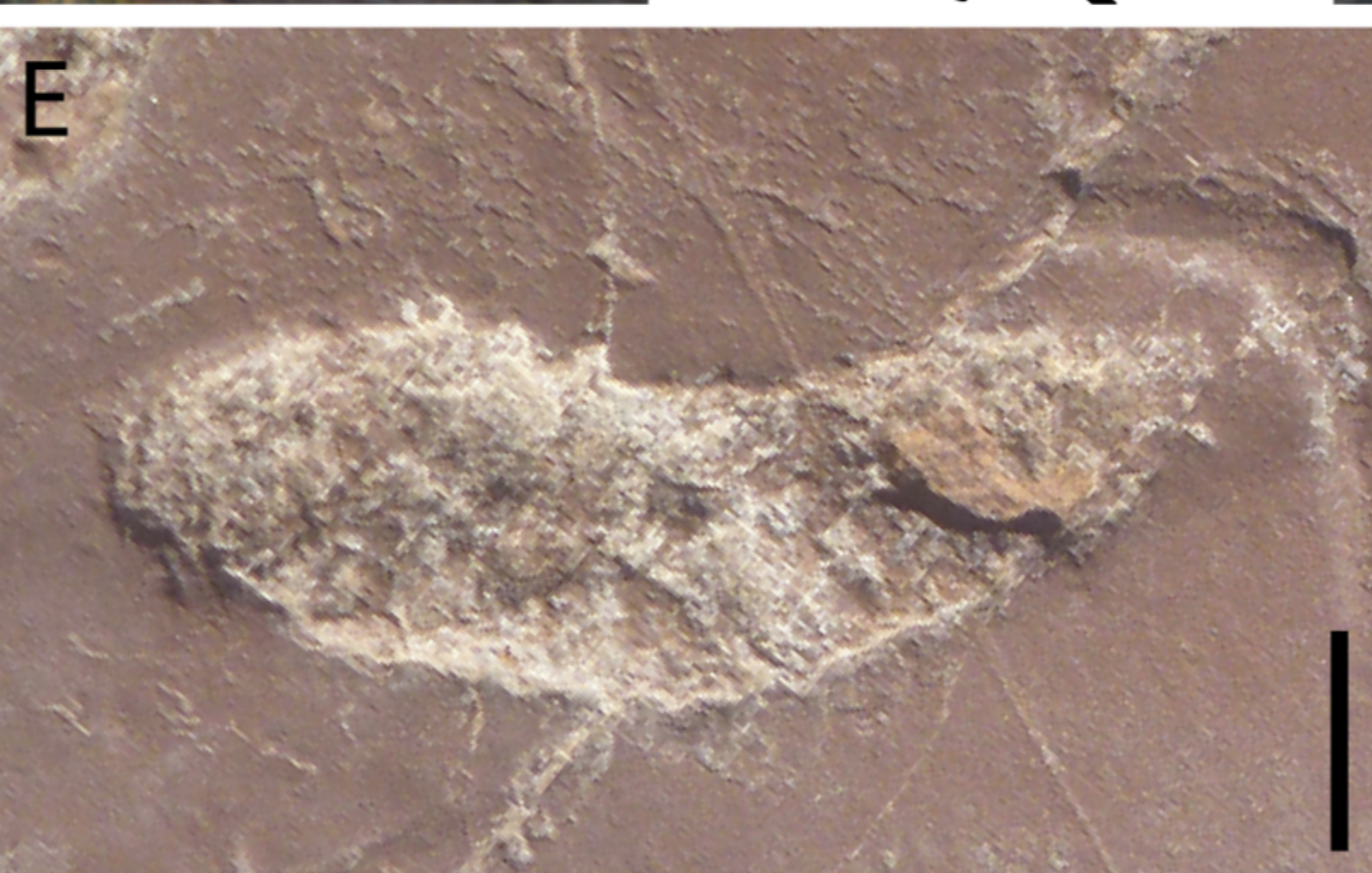
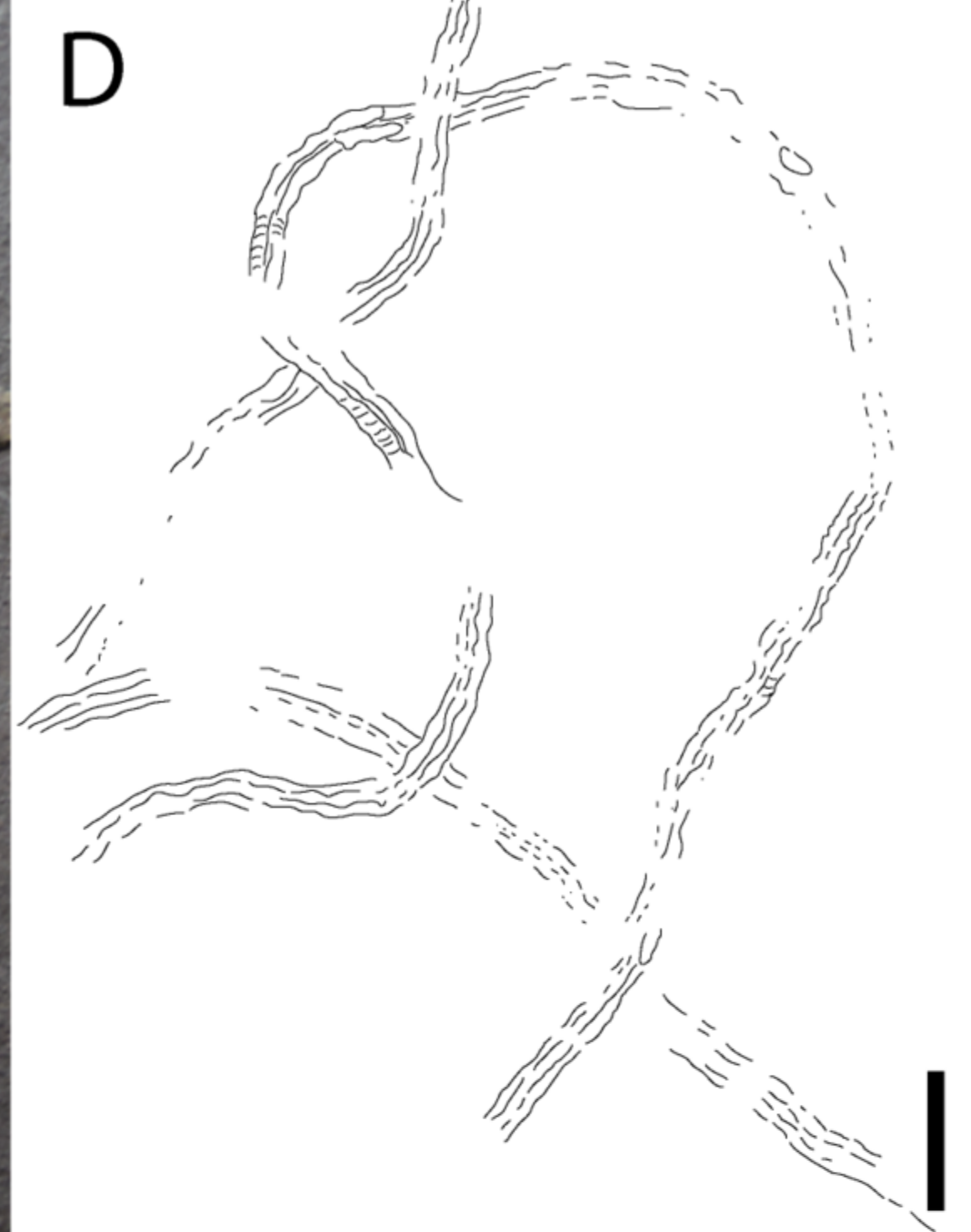
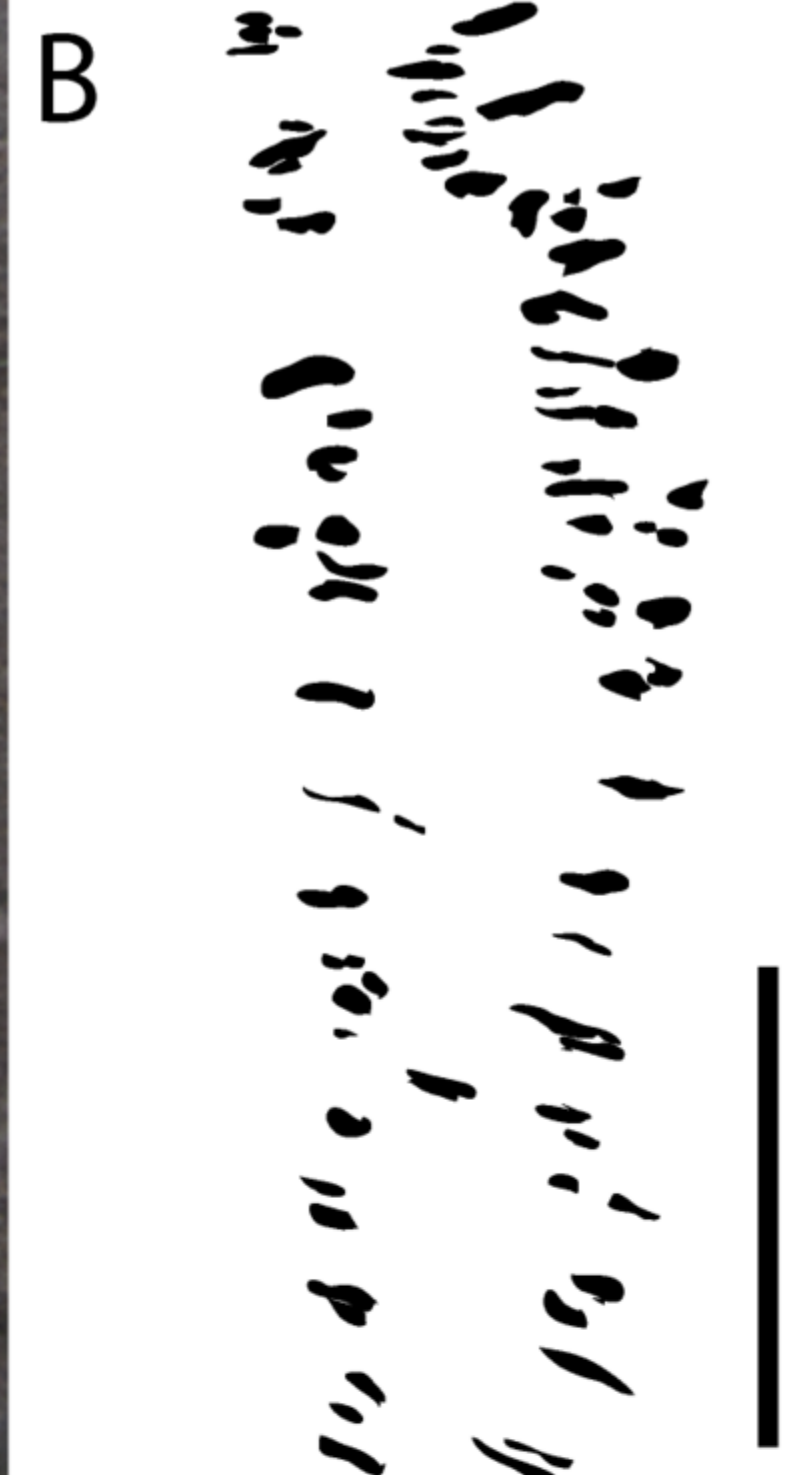
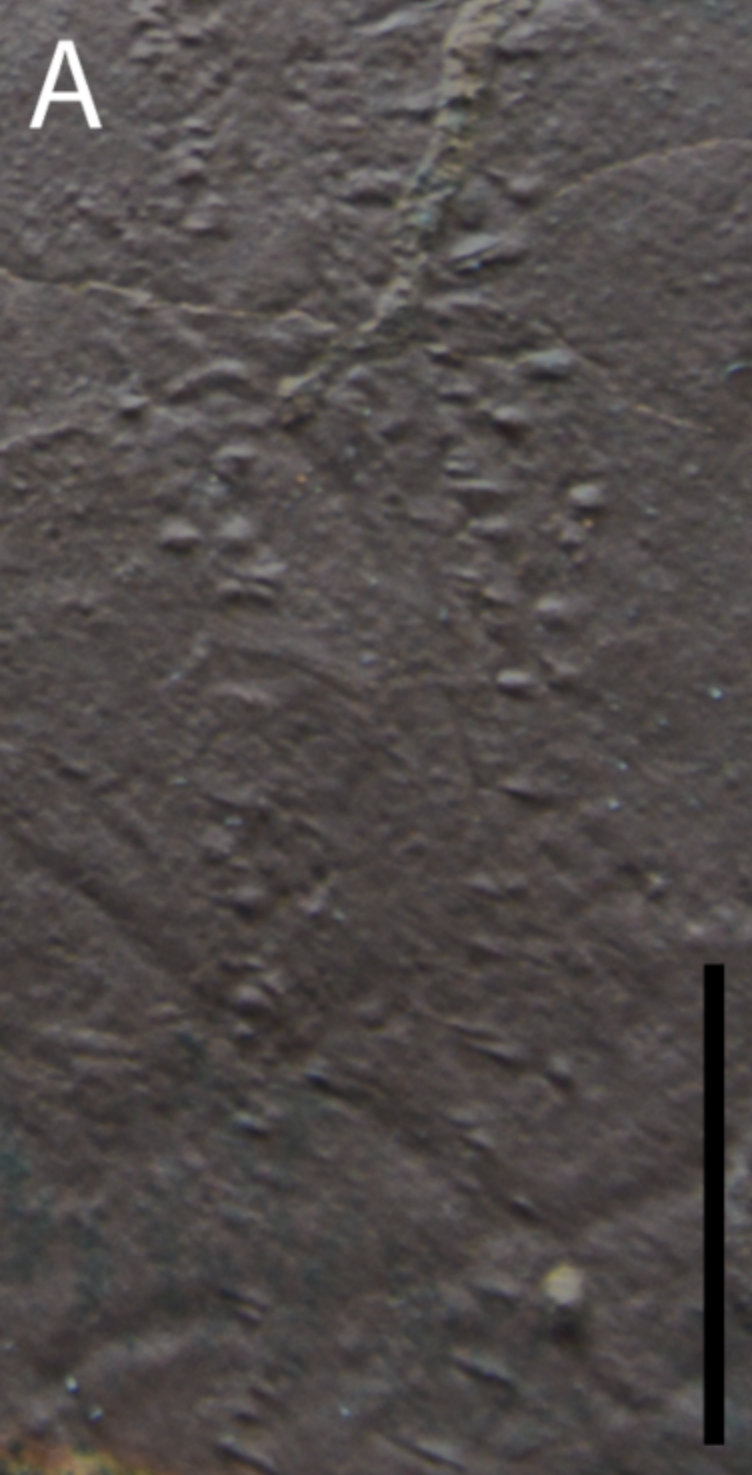
Crinkled 

Mudcracks 

Scoyenia 

Plant remains 

Vertebrate tracks 



A**B****C****D**